CHEMISTRY & CHEMICAL TECHNOLOGY

Chem. Chem. Technol., 2025,
Vol. 19, No. 1, pp. 1–19

Chemistry

PHOTOCATALYTIC SYSTEMS BASED ON CRYSTALLINE CARBON NITRIDE FOR HYDROGEN PRODUCTION

***Stepan Kuchmiy*[1,✉]**

https://doi.org/10.23939/chcht19.01.001

Abstract. The current state of research on photocatalytic systems based on crystalline graphitic carbon nitride (CCN) for H_2 evolution from aqueous solutions of electron-donating substrates is considered. Methods of CCN synthesis and photocatalytic properties of different samples of CCN – undoped with a controlled defect structure and doped with metals and non-metals are discussed. Possible directions for further research of such CCN-based photocatalytic systems are outlined.

Keywords: crystalline carbon nitride, photocatalysis, molecular hydrogen.

1. Introduction

Intensive studies of photocatalytic processes, initiated at the beginning of the 70-s of the last century, continue to arouse considerable interest today. This is due to the attractive prospects of their practical use – for storing solar energy by decomposition of water with the formation of environmentally clean hydrogen fuel,[1,2] fixation of atmospheric nitrogen,[2,3] conversion of carbon dioxide,[1,3,4] for environmental protection environment,[1,5-8] in organic synthesis,[1,9,10] skilled processing of plant biomass with the production of valuable organic substances,[11,12] *etc.* Recently, after the publication of works[13-16] in 2009, materials based on the polymer layered semiconductor of graphite-like carbon nitride ($g\text{-}C_3N_4$) are widely used as photocatalysts of various processes.[17-27] This is due to a number of its valuable properties: $g\text{-}C_3N_4$ can be easily obtained by thermal polycondensation of many nitrogen-containing compounds, it is sufficiently thermally and chemically stable, and partially absorbs visible light, the range of which can be extended by modification. Carbon nitride has a good arrangement of energy zones, which allows you to initiate with its participation photocatalytic oxidation and reduction transformations of many organic and inorganic substrates, in particular, the processes of water decomposition with the formation of hydrogen. However, such material, obtained by thermolysis of precursors, has a small specific surface area, a low concentration of active centers, and an amorphous or partially crystalline structure. In addition, the presence of hydrogen bonds in its framework, which is associated with incomplete deamination of precursors, can impair the electronic conductivity of the material. This leads to rapid recombination of photogenerated charges, so $g\text{-}C_3N_4$ exhibits low photocatalytic activity.

Many approaches to improving the photocatalytic properties of $g\text{-}C_3N_4$ are known: modification using organic compounds, doping with metals and non-metals, increasing the specific surface area and porosity, creating spatially organized structures, nanoheterostructures based on $g\text{-}C_3N_4$, as well as metals and semiconductors of other nature, *etc.*[18,24,25,28-33] A very important factor affecting the photocatalytic properties of carbon nitride is the degree of its crystallinity. With low crystallinity, various defects are usually present in the $g\text{-}C_3N_4$ structure, which can be recombination centers of photogenerated electron-hole pairs. In addition, structural defects are the reason for the imperfection of individual $g\text{-}C_3N_4$ layers and the weak interaction between them. This prevents the rapid release of photogenerated charges to the surface of the semiconductor and slows down the redox transformations of substrate molecules with their participation. Therefore, it is desirable to obtain fully crystalline carbon nitride (CCN).

The layered structure of CCN can be formed using planar subunits based on triazine, tri-s-triazine (heptazine), both of these elements with different contents, as well as structurally similar poly(triazinimide) (PTI), poly(heptazinimide) (PHI) and melon[34] (Fig. 1). Melon consists of heptazine units connected by imide bridges. Melon layers contain polymer chains-ribbons connected by hydrogen bonds with the participation of residual amino groups.[35,36] The composition, structure, and physicochemical properties of the synthesized CCN significantly depend on the nature of the precursor, as well as the method and conditions of synthesis. Different subunits may be present in the actual obtained material, and it is rather difficult to establish its structure.[37]

---

[1] L.V. Pysarzhevsky Institute of Physical Chemistry, NAS of Ukraine, 31 Nauky Ave., 03028 Kyiv, Ukraine

✉ stephan@ukr.net

In the published reviews,[35,37-45] several aspects related to the synthesis and study of the properties of CCN as an active component of photocatalytic systems for various purposes were considered. However, they only partially cover the available data on the application of CCN in water degradation processes. In this regard, this review attempts a more complete analysis of information on the methods of obtaining CCN, its doping with metals and nonmetals, and its properties as a photocatalyst in the hydrogen production reaction. Note that the review does not consider systems for water decomposition involving composite photocatalysts based on CCN and semiconductors of different nature, which may be the subject of a separate review.

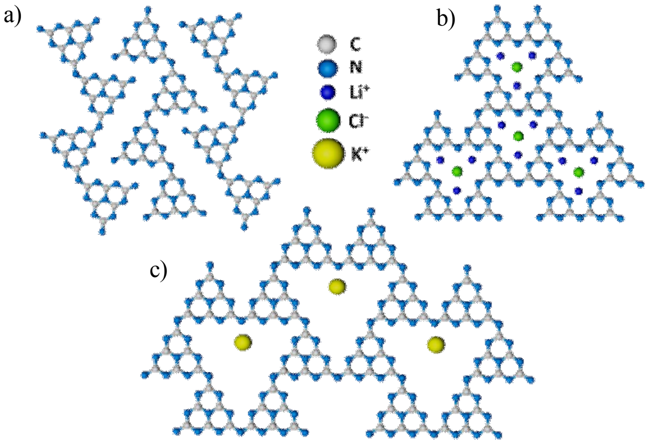

Fig. 1. Idealized structures of carbon nitride based on melon (a), poly(triazinimide) (b) and poly(heptazinimide) (c)[34]

2. Principle Diagrams of the Operation of Photocatalytic Systems for Obtaining Hydrogen

Semiconductor (SC) systems of two types are mainly used for photocatalytic separation of hydrogen from water.[1,2] The most attractive one appears to be systems for the complete decomposition of H_2O with the simultaneous production of H_2 and O_2. However, such systems have not yet found widespread use. This is because they can function when using SCs with a valence band potential that exceeds the water oxidation potential of 1.23 V relative to a normal hydrogen electrode (NHE) at pH 0, and a conduction band potential that is more negative than the NHE potential. At the same time, there are relatively few photoactive SCs that would satisfy these conditions. In addition, under the influence of light, very active primary particles are formed in such systems – a hydrogen atom, a product of the reduction of water molecules by photogenerated electrons, and a hydroxide radical – a product of the oxidation of H_2O molecules by holes. These radical products can quickly recombine and thereby significantly reduce the overall efficiency of the process. Therefore, today, the so-called sacrificial photocatalytic systems are most often used to obtain hydrogen. In addition to water, they contain electron-donating substances, which act as acceptors of photogenerated holes in SC. This significantly slows down the recombination of photogenerated charges and contributes to the increase in the rate of reduction of H_2O molecules by photogenerated electrons with the participation of co-catalysts. The mechanism of obtaining H_2 in semiconductor photocatalytic systems can be represented by the following general scheme:[2]

$$\mathrm{SC} + h\nu \rightarrow \mathrm{SC}\ (e^-_{\mathrm{CB}} \ldots h^+_{\mathrm{VB}}) \tag{1.1}$$

$$e^-_{\mathrm{CB}} \rightarrow e^-_{\mathrm{tr}} \tag{1.2}$$

$$h^+_{\mathrm{VB}} \rightarrow h^+_{\mathrm{tr}} \tag{1.3}$$

$$e^-_{\mathrm{tr}} + \mathrm{Me} \rightarrow \mathrm{Me}(e^-) \tag{1.4}$$

$$\mathrm{Me}(e^-) + \mathrm{H_3O^+} \rightarrow \mathrm{H_2} + \mathrm{OH^-} \tag{1.5}$$

$$h^+_{\mathrm{tr}} + \mathrm{R} \rightarrow \text{products,} \tag{1.6}$$

where equation (1.1) describes the generation of an electron-hole pair under the action of light quanta on SC, (1.2) and (1.3) – capture of an electron and hole by surface traps, (1.4) – transfer of electrons to a metal co-catalyst, (1.5) – recovery of protonated water molecules on its surface, (1.6) – hole oxidation of donor substrates (R) with the production of products of their mineralization or selective transformation into valuable substances.

3. Methods of Obtaining Crystalline Carbon Nitride

Many chemical and physical methods of obtaining g-C_3N_4, including its crystalline forms, are known. Analysis and discussion of methods for the synthesis of CCN, not related to its use in photocatalysis, can be found in the literature.[46-48] Here, we will give only examples of different methods of obtaining CCN, mainly as a photocatalyst for the decomposition of water with the formation of hydrogen.

3.1. Synthesis of CCN at High Temperature

Improving the crystallinity and increasing the photocatalytic activity of g-C_3N_4 can be achieved by increasing the synthesis temperature.[49-51] Thus, a sample of crystalline carbon nitride GS-CN_{700}/Pt was obtained by pyrolysis of guanidine thiocyanate at a temperature of 700 °C.[50] With the participation of a co-catalyst, deposited *in situ* Pt nanoparticles (Pt NPs), CN_{700}/Pt showed 7 times higher photocatalytic activity in the process of H_2

evolution from aqueous solutions of triethanolamine (TEOA) (Table 1) than g-C_3N_4 synthesized at 550 °C. GS-CN_{700} was significantly more crystalline, had fewer defects, and also had a higher specific surface area and photosensitivity in the visible range of the spectrum due to the appearance of an absorption band near 500 nm associated with an n→π* electronic transition involving lone pairs of nitrogen atoms in the heptazine units. Such a transition is forbidden for planar structures; its occurrence indicates that, at a high synthesis temperature, polymer layers of carbon nitride undergo distortion.

For the synthesis of CCN with a developed surface, the polymerization of melamine was carried out in two stages.[52] In the first stage, the precursor was calcined at 400 °C in an N_2 atmosphere, and then the obtained product was calcined under vacuum conditions at 550 °C in the presence of CuO, MnO_2, or Fe_2O_3 to decompose the formed NH_3. This contributed to the polycondensation of melamine and prevented the carbonization of polymer layers of carbon nitride. In the presence of Pt NPs, the CCN samples obtained in this way showed activity in the process of obtaining H_2 (Table 1) – significantly higher than g-C_3N_4 synthesized by the traditional method or samples obtained in the absence of metal oxides.

Highly crystalline nanosheets of carbon nitride CCNNS were obtained by two-stage calcination at high temperatures (Fig. 2).[53] First, bulk g-C_3N_4 was synthesized by polycondensation of dicyandiamide at 520 °C, which was calcined at 620 °C in an argon atmosphere. The obtained CCNNS in the presence of *in situ* precipitated Pt NPs exhibited photocatalytic activity in the process of H_2 evolution from aqueous TEOA solutions (Table 1). The better photocatalytic properties of CCNNS, compared to g-C_3N_4, were due to a more perfect crystalline structure, a larger specific surface area, and a more intense absorption of light in the visible range of the spectrum due to the appearance of an absorption band near 500 nm.

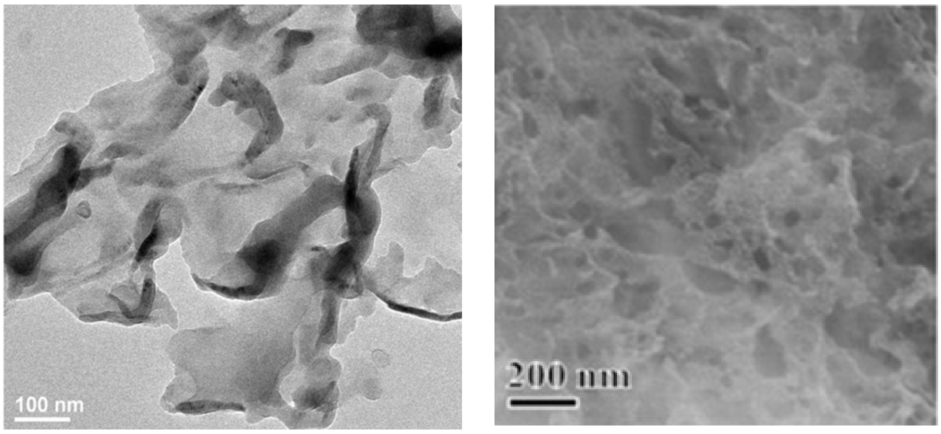

a) b)

Fig. 2. TEM (a) and SEM (b) images of nanosheets CCNNSs[53]

3.2. Synthesis of CCN at High Pressure

Crystalline carbon nitride was obtained by thermal polycondensation of dicyandiamide (DCDA) in an autoclave, which led to the creation of a reaction medium under high pressure.[54] The synthesis of carbon nitride under such conditions contributed to the improvement of its crystallinity, the reduction of the number of defects, the convergence of carbon nitride layers, and the increase of the distance between polymer chains in its plane due to the breaking of hydrogen bonds. The latter led to a partial deterioration of the planarity of the layers and led to the expansion of the CCN light absorption range due to the partial elimination of the prohibition of the n→π* electronic transition involving unshared pairs of nitrogen atoms. The HP550 sample, synthesized in an autoclave at 550 °C, showed almost an order of magnitude higher photocatalytic activity in the process of H_2 evolution from aqueous TEOA solutions than carbon nitride obtained by the traditional method. The apparent quantum yield of H_2 formation with the participation of HP550 in the presence of Pt NPs was $\Phi = 1.6\%$ at $\lambda = 420$ nm (Table 1).

3.3. Preparation of CCN by Microwave Thermolysis

To obtain CCN by this method, melamine[55] or pre-synthesized supramolecular aggregates (microspheres) of melamine with cyanuric acid[56] were baked in a microwave oven in a crucible placed in CuO powder to absorb microwave radiation and rapidly increase the reaction temperature. Compared to g-C_3N_4, synthesized by the traditional method, samples CN16[56] and MCN$_{1000\text{-}18}$[55] obtained by microwave thermolysis were significantly more crystalline, absorbed visible light more intensely, contained fewer structural defects, and showed higher activity in the process of obtaining H_2 from aqueous of TEOA solutions (Table 1) than g-C_3N_4.

3.4. Synthesis of CCN by the Template Method

It was possible to improve the crystallinity of carbon nitride during the synthesis of its nanorods by thermal condensation of DCDA inside channels of anodized aluminum oxide as a template.[57] For the synthesis of CCN, nickel foam was also used as a template, the pores of which were filled with dicyandiamide.[58] After calcination of the modified Ni foam at 550 °C, it was etched with hydrochloric acid, and 2D HC-CCN nanosheets active in the reaction of H_2 evolution from aqueous TEOA solutions were obtained (Table 1). When heated, DCDA in a vapor state underwent condensation with deposition of carbon nitride on the surface of the template. In addition, the Ni foam accelerated the dehydrogenation of amino groups, improved crystallinity, and reduced the number of structural defects.

Table 1. Systems for H_2 evolution from aqueous solutions of electron-donating substrates with the participation of photocatalysts (PC) based on CCN obtained by various methods

PC	S, m^2/g	E_g, eV	Substrate	λ, nm	V, mM/h·g_{PC}	Φ, %	Ref.
GS-CN$_{700}$/Pt	42	2.89	TEOA	> 420(1)	3.44		50
CCN$_{CuO}$/Pt	38	2.73	TEOA	> 300(1)	1.78		52
CCN$_{MnO2}$/Pt					1.76		
CCN$_{Fe2O3}$/Pt					1.78		
CCNNS/Pt	34	2.23	TEOA	> 300(1)	9.577	9.01	53
HP550/Pt	6.2	2.7	TEOA	> 420(2)	0.772	1.6	54
MCN$_{1000\text{-}18}$/Pt	77	2.7	TEOA	> 420(2)	2.0	5.6	55
CN16/Pt	45.3	2.7	TEOA	> 420(1)	2.02		56
HC-CCN/Pt	39.24	2.92	TEOA	> 400(1)	0.808	6.17	58
PTI/KCC/Pt	177		TEOA	> 385(1)	1.32	22.1	59
KPCN/Pd	10	2.7	Methanol	> 420(3)	1.6	7.3	60
CPCN/Pt	13.5	2.71	TEOA	> 420(1)	1.356	11.4	61
NK-PHI/Pt	33.8	2.62	TEOA	> 420(1)	2.161	2.32	34
PHI-K/Pt	10.3	2.71	TEOA	> 420(1)	22.23	3.39	62
Box-KCCN/Pt	4.6	2.50	TEOA	> 420(1)	1.948	2.09	63
Box-NaCCN/Pt	5.3	2.59			0.758	1.03	
PC-CN/Pt	15.34	2.7	Lactic acid	420(4)	1.01		64
HC-CN/Pt	13.6	2.24	Lactic acid	420(4)	0.789	1.2	65
HTCN/Pt	180	2.66	TEOA	> 300(1)	5.764	3.57	68
HBCN/Pt	160	2.99			4.207		
TBCN/Pt	108	2.69			0.378		
PTI/Li^+Cl^-	37		TEOA	> 420(1)	0.864	0.6	70
SPP-MS-CCN/Pt	62.5	2.7	TEOA	>400(1)	1.785	24.3	72
CCNHS/Pt	186	2.72	Bisphenol A	> 320(3)	0.151	1.53	73
			Lactic acid		0.22	3.4	
			Ethanediamine		0.73	8.1	
			Glycerin		0.84	11	
			TEOA		1.1	15	
uPHIP/Pt	169.6	2.83	TEOA	> 420(1)	0.731		74
CN-HC/Pt	5.0	2.58	TEOA	> 420(1)	6.465	23.8	75
CCN/C/Pt	109		Methanol	> 420(1)	0.689		77
PH/PTI/Pt	35.8	2.46	TEOA	> 420(1)	4.813		78
CPCN/Pt	30.77		TEOA	> 420(1)	1.6	9.7	79
mw-ms-CCN/Pt	25.7	2.65	TEOA	> 420(1)	1.48	10.7	80

Notes: S – specific surface area of the photocatalyst; E_g – the width of the forbidden zone; λ – wavelength of irradiation; V i Φ – rate and apparent quantum yield of hydrogen formation, respectively ($\Phi = 2V \cdot 100/I$, %, where V – rate of H_2 evolution, mole/h, I – light intensity, mole quanta/h). Radiation sources: (1) – Xe lamp, 300 Wt; (2) – Xe lamp, 350 Wt; (3) – Xe lamp, 500 Wt; (4) – 4 LED lamps, 3 Wt.

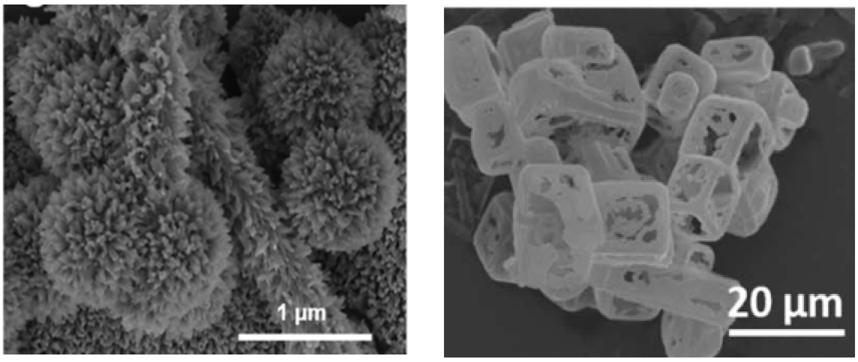

a) b)

Fig. 3. SEM image of PTI/KCC dendritic structures[59] (a) and boxes Box-KCCN[63] (b)

Due to the high crystallinity, the small number of structural defects, and the effective separation of photogenerated charges, the obtained material showed 20 times higher photocatalytic activity than g-C_3N_4, synthesized by conventional thermal condensation of DCDA.

High activity as a photocatalyst for hydrogen evolution from TEOA solutions was demonstrated by crystalline carbon nitride based on polytriazinimide with a PTI/KCC dendritic structure (Fig. 3a), obtained by calcination of a supramolecular melamine aggregate with 2,4,6-triaminopyrimidine (TAP) in a KCl + LiCl melt in the presence of porous fibrous SiO_2 spheres.[59] Under optimal conditions, hydrogen was formed with a quantum yield of Φ = 22.1% under light irradiation with λ = 400 nm (Table 1), which is significantly higher than with the participation of bulk g-C_3N_4. According to theoretical calculations, doping with TAP led to the inclusion of C in the PTI structure. This led to a change in the potentials of the allowed zones of carbon nitride, a decrease in the band gap, and an improvement in the absorption of light in the visible range of the spectrum. In addition, the obtained materials had a larger specific surface area and were characterized by a lower recombination rate of photogenerated charge carriers, which improved their photocatalytic properties.

Highly crystalline carbon nitride with potassium cations intercalated in its structure (KPCN) was synthesized by thermal condensation of melamine in the presence of solid KBr as a salt template.[60] With the participation of KPCN and photodeposited palladium, H_2 evolved from methanol solutions under the influence of visible light with a quantum yield of Φ = 7.23% at λ = 420 nm (Table 1). An efficient hydrogen production photocatalyst CPCN (Table 1) was obtained in the same way using KCl as a solid template to control CCN growth.[61]

Nanostructured potassium poly(heptazinimide) (NK-PHI), as a photocatalyst for obtaining H_2 (Table 1), was synthesized by calcining melamine in the presence of KCl and $Mg(OH)_2$.[34] The water vapor formed during the decomposition of $Mg(OH)_2$ served as a gas template and contributed to the formation of K-PHI nanoparticles. The activity of NK-PHI with the participation of deposited *in situ* Pt NPs was 38.4 and 3.4 times higher than that of bulk g-C_3N_4 and K-PHI obtained in the absence of $Mg(OH)_2$. The synthesis of PHI was also carried out by calcining a mixture of melamine with KCl in the presence of KOH. This led to deeper deamination and expansion of the PHI π-conjugation region.[62] The photocatalytic activity of the obtained PHI-K in the process of hydrogen formation (Table 1) exceeded the activity of the sample synthesized in the absence of alkali by 18 times. Such photocatalytic properties of NK-PHI and PHI-K are associated with their better crystallinity and more efficient separation of photogenerated charges.

Sufficiently active in the process of producing H_2 (Table 1) were samples of CCN based on heptazine doped with potassium or sodium, with a box-like morphology Box-KCCN (Fig. 3b) and Box-NaCCN, synthesized by vapor phase deposition of the formed carbon nitride on microcrystals of KCl or NaCl, followed by their removal by washing with water.[63] Better photocatalytic properties of the obtained crystalline materials were due to more efficient separation of photogenerated charges, as well as more intensive absorption of light in the visible range of the spectrum due to multiple reflection and absorption inside the boxes.

Porous crystalline CCN nanosheets were synthesized by calcination at 550 °C of $NaHCO_3$/DCDA composite, followed by hydrothermal treatment of the obtained material.[64] CO_2 released when $NaHCO_3$ was heated served as a gaseous template for the formation of porous semi-polymerized DCDA. Then, the $NaHCO_3$ – Na_2CO_3 decomposition product served as a high-temperature solvent, where the crystallization of heptazine subunits took place with the formation of porous CCN. The PC-CN/Pt material synthesized by this method turned out to be a sufficiently effective photocatalyst for obtaining H_2 from aqueous solutions of lactic acid (Table 1). Its activity was two times higher than that of bulk g-C_3N_4.

Similarly, CCN was obtained using sodium acetate, which prevented the sublimation of DCDA and intermediate synthesis products.[65] The HC-CN sample obtained under optimal conditions showed 2.4 times higher photocatalytic activity in the process of H_2 evolution from aqueous solutions of lactic acid than the usual g-C_3N_4. This was facilitated by a highly crystalline structure, a smaller band gap, and the presence of defects – cyano groups, which could capture electrons and thereby improve the separation of photogenerated charges.

3.5. Solvothermal Synthesis of CCN

Highly ordered CCN with surface defects – cyanide and carboxyl groups – was synthesized by the solvothermal method.[66] An acetonitrile solution of a mixture of guanidine hydrochloride and DCDA was kept in an autoclave at 180 °C for 2 days, the obtained sheet-like CCN was purified by dialysis and dried. Compared to conventional g-C_3N_4, CCN more intensively absorbed light in the visible range of the spectrum and had higher electrical conductivity, which contributed to the separation of photogenerated charges. In addition, CCN was able to accumulate electrons, which collectively determined its high photocatalytic activity in the process of reducing CO_2 with water vapor.

3.6. Ionothermic Synthesis of CCN

This method, proposed in the literature,[67] which is also called the molten salt method, is now most often used to obtain photocatalytically active CCN samples. According to this method, the synthesis of CCN is mainly carried out in two stages. In the first stage, the usual thermal condensation of the precursors is carried out, and in the second stage, the obtained product is additionally processed at a high temperature in the eutectic melt of salts (KCl + LiCl, NaCl + KCl, *etc.*). Such heat treatment of primary g-C_3N_4 is usually accompanied by the introduction into its structure of cations and anions that are part of salts, as well as other functional groups.

CCN samples can be formed by the ionothermal method with the participation of different planar subunits – polytriazine, polyheptazine, or both of these elements with the formation of polytriazine/polyheptazine heterostructures. Thus, after heat treatment in a melt salts of KCl + LiCl g-C_3N_4, synthesized by condensation of melamine at 450 ^{o}C, CCN based on polyheptazine (HBCN) with a coral-like structure consisting of nanorods was obtained (Fig. 4b).[68] When using carbon nitride synthesized by the calcination of melamine, treated with an H_2SO_4 solution, after its heat treatment in a KCl + LiCl melt in a nitrogen atmosphere, CCN based on polytriazine (TBCN) was obtained in the form of aggregated blocks (Fig. 4a), and in an air atmosphere – heterostructure polyheptazine/ polytriazine (HTCN). All the obtained materials had a large specific surface, and in the presence of deposited *in situ* Pt NPs, hydrogen was released from aqueous TEOA solutions under the action of light (Table 1). The highest efficiency was demonstrated by HTCN/Pt with a type II heterojunction formed at the boundary of the HBCN and TBCN phases (Fig. 4c), which ensured a better separation of photoenerated charges. HBCN/Pt also exhibited sufficiently high activity due to the presence of cyano groups in its structure, which also contributed to the separation of electron-hole pairs. Hydrogen evolved at the lowest rate with TBCN/Pt, which may be due to poorer charge mobility in TBCN compared to heptazine-based materials.

The ionothermal method of CCN synthesis has undergone some other modifications. In particular, a eutectic salt solvent was used at both stages of synthesis. In this way, PTI with lithium and chlorine ions introduced into its structure (PTI/Li^+Cl^-)[67,69,70] was obtained in the molten mixture of KCl + LiCl. The synthesized material showed activity under the influence of light in the process of H_2 evolution from aqueous solutions of TEOA (Table 1).[70] Photocatalytically active crystalline PTI/Li^+Cl^- was obtained by calcination of DCDA at 600 °C in the presence of only lithium chloride.[71]

Hollow tubes with a crystalline structure based on triazine and heptazine were obtained by the one-step molten salt method by thermal condensation of melamine in the presence of sodium polyphosphate.[72] The obtained SPP-MS-CCN nanomaterial (Fig. 5a) with the optimal ratio of these structural units demonstrated, in the presence of *in situ* deposited Pt NPs, high activity in the process of hydrogen evolution from aqueous TEOA solutions with a quantum yield of $\Phi = 24.3\%$ at $\lambda = 420$ nm (Table 1), which was 14.5 times higher than with the participation of bulk g-C_3N_4. This was due to a larger specific surface area of nanotubes, better separation and transfer of photogenerated charges, as well as a higher reduction potential of the material's conduction zone.

Using the same method, highly crystalline hollow spheres of carbon nitride CCNHS (Fig. 5b) formed by polymer links of heptazine and triazine were obtained.[73] Their synthesis was carried out using a complex of cyanuric acid with melamine as a precursor. Along with high crystallinity, the CCNHS samples had a large specific surface area and a significant number of surface defects, which played the role of active sites in photocatalytic processes. In addition, the presence of two isotypes of carbon nitride in the samples led to the formation of a type II heterojunction, which contributed to the separation of photogenerated charges. Thanks to the combination of these properties, the synthesized hollow spheres of carbon nitride turned out to be active photocatalysts for H_2 evolution from aqueous solutions of various electron-donating substrates – bisphenol A plasticizer, lactic acid, glycerol, ethanediamine, and TEOA (Table 1).

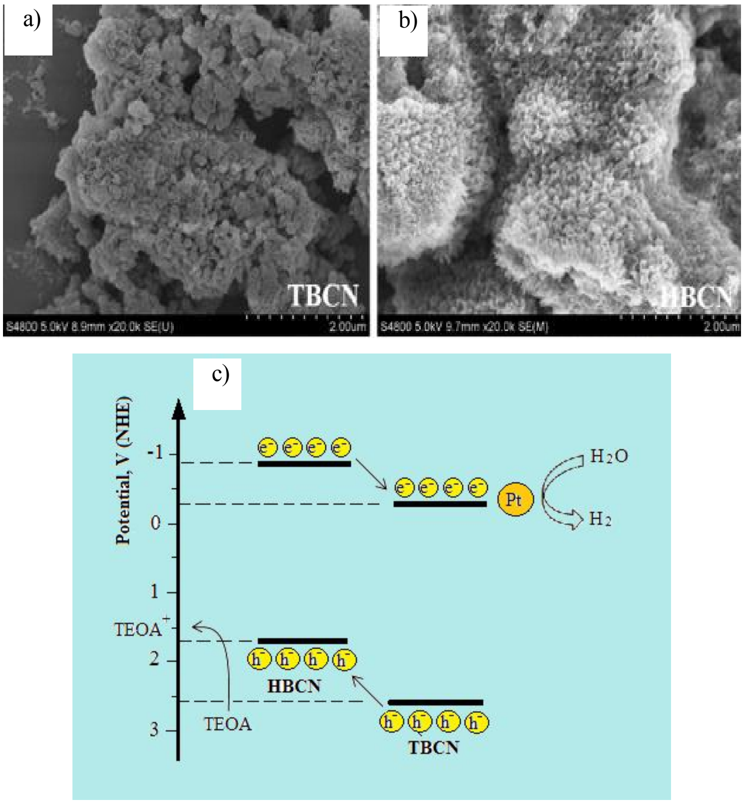

Fig. 4. SEM images of TBCN (a), HBCN (b), and a probable scheme of the mechanism of the photocatalytic process involving the HTCN heterostructure[68]

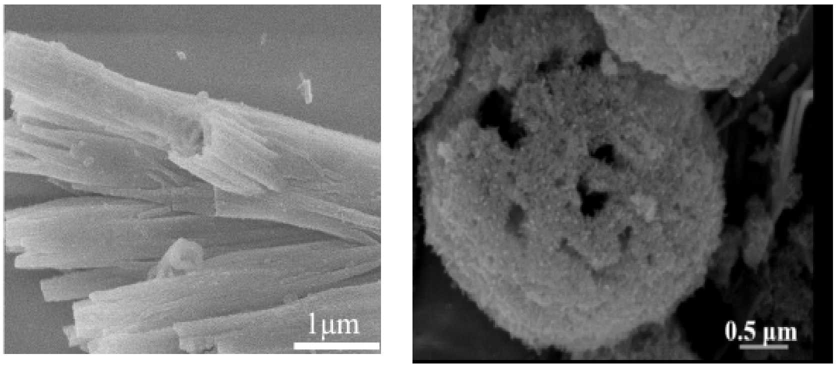

a) b)

Fig. 5. SEM image of SPP-MS-CCN hollow tubes[72] (a) and hollow spheres CCNHS[73] (b)

CCN was also synthesized in three stages.[74] First, a melon was obtained by condensation of urea at 500 °C, which was heated at the same temperature for 2 h to increase crystallinity and, finally, calcined at 500 °C (2 h) in a melt salts of KCl + LiCl + NaCl. Synthesized polyheptazinimide (uPHIP) in the presence of deposited *in situ* Pt NPs demonstrated photocatalyst properties for H_2 evolution from TEOA solutions (Table 1). Due to better crystallinity, fewer defects, more efficient separation of photogenerated charges, and a large specific surface area, the activity of uPHIP was 3.8 times higher than that of the sample obtained without additional heating.

The three-stage ionothermic method of CCN synthesis was used by Wang *et al.*[75] Initially, a supramolecular intermediate was obtained by hydrothermal treatment of the DCDA solution at 180 °C, which was subjected to pyrolysis in air at 550 °C. The synthesized porous carbon nitride (CN-HA) was treated in a melt salts of KCl + NaCl to obtain crystalline carbon nitride (CN-HC). Due to its high crystallinity, CN-HC showed much higher activity in the process of H_2 evolution from TEOA solutions than bulk g-C_3N_4 and CN-HA with a much larger specific surface area (S = 73.9 m^2/g). With the participation of CN-HC/Pt, hydrogen evolved with a quantum yield of $\Phi = 23.8\%$ at $\lambda = 420$ nm (Table 1).

According to a slightly different three-step procedure, CCN was synthesized by Yu *et al.*[76] At the first stage, partial condensation of melamine was carried out at 500 °C, then the product was calcined at 550 °C in a melt salts of KCl + LiCl, and additionally heated at 550 °C in an N_2 atmosphere in the presence of NaSCN + NH_4Cl salts. CCN synthesized by this method and functionalized with amine and cyanide groups showed 5 times higher photocatalytic activity in the process of obtaining hydrogen than g-C_3N_4 obtained by the traditional method.

A composite photocatalyst based on CCN and conductive carbon black (CCN/C/Pt) was obtained by one-step calcination at 500 °C of a mixture of melamine and carbon black in a NaCl + KCl + LiCl melt.[77] Due to better separation of photogenerated charges and their transport, the synthesized composite demonstrated photocatalytic activity in the process of obtaining H_2 from aqueous solutions of methanol and TEOA (Table 1), which was higher than in the absence of carbon black. Polyheptazine/polytriazinimide (PH/PTI) heterostructures were synthesized using the same one-step method – urea condensation in a KCl + LiCl melt.[78] In the presence of *in situ* precipitated Pt NPs PH/PTI showed high activity in the process of hydrogen evolution from aqueous TEOA solutions (Table 1).

3.7. Other Approaches to Obtaining of CCN

In addition to the above-described methods for the synthesis of CCN, some other approaches for its preparation have been proposed. Thus, in the literature[79] CCN was synthesized by one-step calcination of melamine with KOH and NH_4Cl at different ratios. At a low NH_4Cl content, CCN samples were obtained with a good arrangement of their planes, and at a high content – with better stacked layers. In the presence of deposited *in situ* platinum, all synthesized materials (CPCN/Pt) absorbed light more intensively and showed sufficiently high activity in the process of obtaining hydrogen (Table 1) – higher than bulk g-C_3N_4.

CCN was synthesized by polymerization of melamine in melt salts of KCl + LiCl using microwave heating.[80] The obtained mw-ms-CCN material with lamellar morphology was constructed with the participation of triazine and heptazine polymer chains. In the presence of *in situ* deposited Pt NPs, mw-ms-CCN showed the activity in the process of obtaining hydrogen (Table 1), which was significantly higher than when using the bulk g-C_3N_4, as well as samples synthesized using only microwave or ionothermic methods. Such properties of mw-ms-CCN were due to the formation of a type II heterojunction at the polytriazine/polyheptazine phase boundary, which contributed to the transfer of charge carriers and a more efficient separation of photogenerated electron-hole pairs than in other samples.

4. Optimization of Photocatalytic Properties of Crystalline Carbon Nitride

4.1. Regulation of Defective Structure

As mentioned above, an increase in the degree of crystallinity of g-C_3N_4 leads to an increase in its photocatalytic activity due to an increase in the speed of movement of charges and their more efficient separation, as well as a decrease in the number of defects in the volume of the material, which are the recombination centers of photogenerated electrons and holes. At the same time, the latter process is facilitated by the presence in the structure of the material of vacancies of various natures, which act as traps for photogenerated charges. Particularly important for photocatalytic activity are surface vacancies – active centers, with the participation of which redox transformations of substrate molecules take place. In addition, such defects in the structure of the material lead to the formation of impurity energy levels inside the band gap, which expands the range of its photosensitivity. Therefore, an effective photocatalyst should be characterized by an optimal ratio of crystallinity and density of structural defects[37,41,43]

Typical structural defects are carbon and nitrogen vacancies, incompletely condensed amine groups, as well as cyanide and other functional groups that can be formed during synthesis. The presence of cyanide and other functional groups can be detected using infrared and X-ray fluorescence spectroscopy, and evidence of the presence of carbon or nitrogen vacancies in the structure of carbon nitride is a significant deviation from the stoichiometry of carbon and nitrogen content in the obtained material. It should be noted that when using different methods of synthesis of carbon nitride, the content of these elements in it, in most cases, does not correspond to the theoretical one. For example, nitrogen vacancies were formed during the synthesis of crystalline carbon nitride by a two-stage ionothermic method – heat treatment in a KCl + LiCl melt of bulk g-C_3N_4 synthesized by pyrolysis of melamine[81]. The obtained g-C_3N_x with nitrogen vacancies showed photocatalytic properties in the presence of Pt NPs in the process of H_2 evolution from TEOA solutions (Table 2).

Its activity was 2.2 times higher than that of g-C_3N_4, which is attributed to the synergistic effect of a higher degree of polymerization, better crystallinity, smaller band gap, and more efficient separation of photogenerated charges, which was facilitated by the formed nitrogen vacancies and cyanide functional groups.

Different approaches can be used to purposefully introduce structural defects into carbon nitride. Thus, a composite with carbon vacancies based on isotypes of carbon nitride – melon and polyheptazinimide (melon-PHI) was synthesized by the hydrothermal method.[82] The obtained material in the presence of Pt NPs demonstrated the properties of a photocatalyst of simultaneous hydrogen evolution and selective oxidation of 5-hydroxymethylfurfural to 2,5-dimethylfuran. According to theoretical calculations, carbon vacancies in defective heptazine rings in PHI contribute to increasing the charge density on the highest occupied molecular orbital of the composite, improving the separation of photogenerated electron-hole pairs and the efficiency of photocatalytic redox reactions.

Table 2. Systems for H_2 evolution from aqueous solutions of electron-donating substrates with the participation of photocatalysts (PC) based on CCN with a defective structure

PC	S, m^2/g	E_g, eV	Substrate	λ, nm	*V*, $mM/h{\cdot}g_{PC}$	*Φ*, %	Ref.
g-C_3N_x/Pt	48.35	2.64	TEOA	> 420$^{(1)}$	0.403		81
D-CCN/Pt	58	2.63	TEOA	> 455$^{(1)}$	1.28	12.9	83
CNCN/Pt		2.59	TEOA	> 420$^{(1)}$	3.591	8.3	84
g-C_3N_4-D/Pt		2.37	Lactic acid	> 400$^{(2)}$	0.668	8.78	85
g-C_3N_4-D/Pt/Co_3O_4					3.78	11.94	
DCN/Pt	48.2	2.60	TEOA	> 420$^{(1)}$	1.209		86
ODH-CN/Pt	108.2	2.61	TEOA	> 420$^{(1)}$	5.833		87
			TC-HCl		0.591		
			SMZ		0.397		
CCN/Pt	43.8	2.08	TEOA	> 420$^{(1)}$	3.417	10.71	88
KCN_x/Pt	58.5	2.72	TEOA + NaCl	> 420$^{(1)}$	59.9	57.17	89
CCN/Pt	23.47	2.43	Lactic acid	420$^{(3)}$	0.759	1.17	90
CCN/Pt	31.25	2.21	TEOA	> 420$^{(1)}$	4.0	14.65	91
KC-CCN/Pt		2.38	TEOA	> 420$^{(1)}$	4.125		92
CC-CN/Pt	103		Methanol	420$^{(3)}$	5.906	12.61	93
CN-M-NKH/Pt	7.15	2.74	Methanol	>350$^{(1)}$	10.78	24.5	94
CCN/Pt	65.2	2.31	TEOA	> 420$^{(1)}$	2.69	11.2	95
			TEOA + NaCl		11.0	42	
Na-PHI/Pt			TEOA + LiCl	> 420$^{(4)}$	5.33	13	96
DCN-NaK-ABN/Pt	34.1	2.68	TEOA	> 420$^{(1)}$	6.08		97
				500$^{(1)}$	0.88	8.15	
				550$^{(1)}$	0.50	4.01	

Notes: Radiation sources: $^{(1)}$ – Xe lamp, 300 Wt; $^{(2)}$ – LED lamp, 5 Wt; $^{(3)}$ – 4 LED lamps; $^{(4)}$ – white LED, 50 Wt. Other designations are the same as in the table. 1.

To obtain a photocatalyst with nitrogen vacancies, CCN, synthesized by the two-stage molten salt method, was subjected to heat treatment with the reductant $NaBH_4$ in an inert atmosphere.[83] The D-CCN formed in this way showed activity in the process of hydrogen evolution from aqueous TEOA solutions under the influence of light of the visible spectral range – up to λ = 610 nm (Table 2), which was 7 times greater than with the participation of unmodified CCN. Such properties of D-CCN were due not only to its high crystallinity and better separation of photogenerated charges but also to the formation of defective energy states inside the band gap, which led to the expansion of the light absorption range.

Crystalline carbon nitride with nitrogen vacancies and cyanide groups (CNCN) was obtained using bulk g-C_3N_4 synthesized by thermal polycondensation of melamine, followed by its calcination in a nitrogen atmosphere at 650 °C and, finally, heat treatment of the mixture of the obtained material with KSCN in an inert atmosphere at 500 °C.[84] The synthesized CNCN demonstrated photocatalytic activity in the H_2 evolution reaction (Table 2), which was 13.6 times higher than when g-C_3N_4 was used due to more intense light absorption in the visible range of the spectrum, better crystallinity, and more efficient separation of photogenerated charges. With the participation of CNCN/Pt, hydrogen evolved with quantum yields Φ = 8.3% at λ = 420 nm and 0.9% at λ = 550 nm.

Water decomposition photocatalysts – samples of carbon nitride with nitrogen vacancies in the form of crystalline nanosheets with an adjustable zone structure (g-C_3N_4-D) were synthesized by a two-stage ionothermic method with heat treatment in the second stage of a mixture of g-C_3N_4 with KOH.[85] g-C_3N_4-D obtained under optimal conditions in the presence of *in situ* deposited Pt NPs released H_2 from aqueous solutions of lactic acid with a quantum yield of Φ = 8.78%, and with the participation of two co-catalysts – Pt NPs and Co_3O_4 nanorods with Φ = 11.94 % at λ = 400 nm (Table 2).

High crystallinity carbon nitride (DCN), rich in nitrogen vacancies, was synthesized by the molten salt method with two-stage treatment with a KOH solution.[86] Due to the large number of surface defects and cyano groups, which contributed to the efficient separation of charges, the DCN photocatalyst demonstrated activity in the process of obtaining hydrogen (Table 2), which was 4.7 times higher compared to bulk g-C_3N_4.

Carbon nitride with nitrogen vacancies and improved crystallinity (ODH-CN) was synthesized by calcining a mixture of urea with oxalyl dihydrazide (ODH).[87] The obtained material was used as a photocatalyst for hydrogen evolution from TEOA solutions, as well as for the simultaneous production of H_2 and the decomposition of tetracycline hydrochloride (TC-HCl) and sulfamethoxazole (SMZ) (Table 2). ODH-CN was significantly more active than g-C_3N_4 obtained in the absence of ODH, which was due to more intense light absorption due to the appearance of the $n \rightarrow \pi^*$ band of the electronic transition in the range of 450-620 nm and better separation and movement of photogenerated charges.

Crystalline carbon nitride based on triazine and heptazine structural units with nitrogen vacancies was obtained by incorporating 2,4-diamino-6-hydroxypyrimidine (DHP) into the framework of bulk g-C_3N_4, followed by its treatment in melt salts of KCl + LiCl + + NaCl.[88] The optimal synthesized sample of CCN was a significantly more active photocatalyst for H_2 evolution from aqueous TEOA solutions under the influence of visible light of a wide spectral range – up to 600 nm (Table 2) than unmodified g-C_3N_4 and CCN. The better functional characteristics of DHP-modified CCN are due to a larger surface area, higher crystallinity, and lower recombination efficiency of photogenerated charges.

An even more active photocatalyst for the release of hydrogen from TEOA solutions in the presence of NaCl was the crystalline carbon nitride KCNx with nitrogen vacancies and potassium ions introduced into its structure, obtained by the two-stage ionothermic method.[89] With the participation of KCN_x, hydrogen evolved with an apparent quantum efficiency of Φ = 57.17% at λ = 420 nm (Table 2). Such properties of KCNx are associated with its large surface area, more intense absorption of light, increased reduction potential of the conduction band, and better separation of photogenerated electron-hole pairs.

A significant role in the formation of an effective photocatalyst is played by such structural defects as terminal cyanide groups, which can be formed in the process of CCN synthesis, which was mentioned above when analyzing the results obtained in the works.[65,76,84] To introduce cyanide groups into the CCN structure, high-temperature calcination of a mixture of DCDA with Na_2CO_3 was performed.[90] At the initial stage of calcination, Na_2CO_3 contributed to the denitrification of DCDA and its polymerization with the formation of a highly crystalline material, and at temperatures above 500 ^oC – partial pyrolysis of s-triazine units with the formation of cyano groups on the surface of carbon nitride. CCN obtained in this way demonstrated photocatalytic properties in the process of obtaining H_2 from aqueous solutions of lactic acid (Table 2), which are significantly better than bulk g-C_3N_4.

Crystalline carbon nitride with cyanamide defects was synthesized using potassium isothiocyanate (KSCN), obtained *in situ* by isomerization of thiourea in the presence of KCl, followed by its interaction at high temperature with amino groups (-NH_2 and -NH) in tri-s-triazine rings with the formation of two types of cyanamide defects.[91] The optimized CCN photocatalyst demonstrated a high rate of H_2 evolution from TEOA aqueous solutions (Table 2) due to intensive light absorption in the visible range of the spectrum and effective separation of photogenerated charges.

To simultaneously introduce cyano groups and potassium ions into the CCN structure, it was synthesized by calcining a mixture of thiourea and potassium thiocyanate.[92] The obtained KC-CCN more intensively absorbed visible light due to the appearance of an absorption band in the range of 480-650 nm, and also more effectively separated photogenerated charges, which determined its sufficiently high activity as a photocatalyst for hydrogen evolution from TEOA solutions (Table 2), which was in 16, 8 times higher than with the participation of bulk g-C_3N_4.

To enrich CCN with cyanide groups, it was additionally treated by heating with ethyl acetate.[93] This led to the ordering of the material structure, the removal of residual K^+ ions, and an increase in the number of grafted cyano groups. The obtained CC-CN was used as a photocatalyst for H_2 evolution from water-methanol solutions (Table 2). Such functional properties of CC-CN are associated with an improved ordered structure and a large number of cyano groups.

Nanosheet CCN with a heptazine structure, modified with potassium ions and cyanamine groups (CN-M-NKH), demonstrated even higher photocatalytic activity in the process of obtaining H_2 from solutions of the same substrate (Table 2).[94] It was prepared by roasting mixtures of melamine with solid salts NaCl + KCl. Then the product was treated with a solution of HCl, which led to the delamination of the material and allowed to regulate the concentration of K^+ and the charge of the formed cyanoamine groups, which facilitated the dissociation of excitons. With the participation of these dopants, solvated electrons generated during irradiation could be stabilized on the surface of the photocatalyst, and the electron capacity increased, which caused its high activity. With the participation of CN-M-NKH, hydrogen evolved with a quantum yield of Φ = 24.5% at λ = 420 nm (Table 2).

CCN in the form of porous nanoribbons with terminal cyanamide groups was synthesized by polymerization of urea in the presence of KCl.[95] The obtained material demonstrated high activity in the process of hydrogen evolution from TEOA solutions (Table 2) due to the intense absorption of light in the visible range of the spectrum due to the appearance of the $n \rightarrow \pi^*$ electronic transition band, as well as the effective separation of photogenerated charges, which was facilitated by the internal electric field. The speed of the process increased significantly when NaCl was added to the reaction mixture. In the presence of NaCl, the surface electron density increased, and adsorbed chlorine ions could act as mediators of photogenerated holes. The quantum yield of hydrogen formation in such a system reached Φ = 42% at λ = 420 nm and Φ = 5% at λ = 520 nm.

An increase in the efficiency of water decomposition with the participation of CCN was observed not only in the presence of NaCl in the reaction mixture[89,95] but also in salts of other alkali metals when using sodium polyheptazinimide (Na-PHI) as a photocatalyst.[96] It was established that the degree of positive influence of alkali metal cations is determined by their hydration energy ($Li^+ > Na^+ > K^+ > Cs^+$) and is associated with the activation of the H-OH bond at the stage of dissociation of water molecules on the surface of the platinum co-catalyst due to the interaction of cations with negatively charged oxygen, as well as with the stabilization of the OH^- anion formed by them. In addition, alkali metal cations can contribute to the transfer of photogenerated electrons to the co-catalyst. Under optimal conditions with the participation of Na-PHI/Pt, hydrogen evolved in the presence of LiCl with a quantum yield of Φ = 13% at λ = 420 nm (Table 2).

By joint thermal polycondensation of DCDA and aminobenzonitrile (ABN) with subsequent calcination in melt salts of NaCl + KCl, crystalline carbon nitride with improved electron delocalization containing nitrogen vacancies and cyanide groups introduced into its structure was synthesized.[97] Under optimal conditions, the obtained DCN-NaK-ABN in the presence of deposited *in situ* Pt NPs exhibited photocatalytic properties in the process of H_2 evolution from TEOA solutions (Table 2). Its activity was sufficiently high when irradiated with light with a wavelength of more than 500 nm due to enhanced optical absorption in the visible range of the spectrum.

4.2. Doping with Metals and Non-Metals

It is known[28] that one of the ways to improve the photocatalytic properties of bulk g-C_3N_4 is its doping with metals and nonmetals, which allows controlling the width of the band gap and the potentials of the allowed zones, influencing the efficiency of separation of photogenerated electron-hole pairs, *etc*. Doping with cations and anions was also used to increase the photocatalytic activity of CCN.

Alkali metals. Crystalline polyheptazinimides of sodium (Na-CN), potassium (K-CN), cesium (Cs-CN), and lithium polytriazinimide (Li-CN) were obtained by the solid-phase reaction of melamine with alkali metal chlorides at 550-600 °C, with subsequent washing of salts with water.[98] All synthesized materials were tested in the presence of deposited *in situ* Pt NPs as photocatalysts for hydrogen evolution from TEOA solutions (Table 3). Li-CN demonstrated the least activity, Na-CN was the most active among polyheptazine imides, which may be due to the more intense absorption of light in the visible range of the spectrum due to the appearance of the $n \rightarrow \pi^*$ electron transition band and its largest specific surface.

A series of samples of potassium-doped heptazine-based crystalline carbon nitride (KCCN) were obtained by calcining mixtures of bulk g-C_3N_4 and KCl at 600 °C for different times.[99] This made it possible to control the diffusion of potassium ions from the surface into the carbon nitride volume and their content in the material structure. As a result of the concentration gradient of potassium ions arising in KCCN, an internal electric field was formed, which, together with the formed cyanide groups, contributed to the dissociation of photogenerated electron-hole pairs. This determined the 34 times higher photocatalytic activity of KCCN in the process of obtaining hydrogen under the influence of visible light (Table 3) compared to bulk g-C_3N_4. The photocatalytic release of hydrogen from methanol solutions was studied with the participation of CCN with potassium ions intercalated in its structure, which was obtained by calcining previously synthesized bulk g-C_3N_4 in a KCl + LiCl melt.[36,100] The CCN samples demonstrated sufficiently high activity under the influence of visible light (Table 3) due to better crystallinity, more intense light absorption, and a lower rate of recombination of photogenerated charges.

Table 3. Systems for H_2 evolution from aqueous solutions of electron-donating substrates with the participation of photocatalysts (PC) based on CCN, doped with metal and non-metal ions

PC	Dopant ions	S, m^2/g	E_g, eV	Substrate	λ, nm	V, mM/h·g$_{PC}$	Φ, %	Ref.
Li-CN/Pt	Li	40	2.78	TEOA	>400$^{(1)}$	0.056		98
Na-CN/Pt	Na	72	2.71	TEOA		1.344		
K-CN/Pt	K	6	2.65	TEOA		0.31		
KCCN/Pt	K	9.4	2.68	TEOA	>420$^{(2)}$	5.24	24.5	99
CCN/Pt	K	115.9		Methanol	>420$^{(2)}$	0.66	6.8	100
CCN/Pt	K	125	2.72	Methanol	>420$^{(2)}$	0.55		36
				Ethanol		0.85		
				TEOA		1.472		
APMCN/Pt	K	12.8	2.62	TEOA	>300$^{(2)}$	10.96	62.8	101
Rb-PCN/Pt	Rb		2.67	TEOA	>420$^{(2)}$	2.14	17.3	102
Cs-CN/Pt	Cs	16	2.68	TEOA	>400$^{(1)}$	0.494		98
CsCN-2h/Pt	Cs	40.82	2.67	TEOA	>420$^{(2)}$	385.6	12.6	103
K–Na–CCN/Pt	K-Na	5.42	2.48	TEOA	>420$^{(2)}$	1.38	1.8	104
CNIC/Pt	Li-K-Na	124	2.71	TEOA	>420$^{(2)}$	3.46		105
				TEOA+KCl+NaCl+LiCl		5.02	21.2	
MKCN/Pt	Mg	9.5		TEOA	>420$^{(2)}$	3.386		106
SKCN/Pt	Sr	12.5				3.508		
CKCN/Pt	Ca	9.9	2.7			5.19	31.2	
BKCN/Pt	Ba	21.2				4.026		
Mg-K-PHI/Pt	Mg		2.71	TEOA	>400$^{(1)}$	0.539	7.14	107
Mg-K-CGCN+Pd/SiO_2	Mg		2.7	Ethanol. HCl	>400$^{(3)}$	5.4	99	108
Zn-CCN/Pt	Zn	54	2.74	Methanol	>420$^{(2)}$	1.5	12.6	109
Zn-K-CN/Pt	Zn-K	32.3	2.13	Methanol	>420$^{(2)}$	1.652	3.5	110
Ni-H/T-CCN/Pt	Ni		2.59	TEOA	>300$^{(2)}$	4.933	7.8	111
Co-CCN/Pt	Co	80.9	2.74	Lactic acid	>420$^{(2)}$	32.1	49.5	112
CNF/SCNF-MS/Pt	S	56.6		TEOA	>420$^{(2)}$	1.421	2.76	113
S-CGCN/Pd	S	23	2.76	Ethanol. HCl	>400$^{(3)}$	3.0	99	114
B-CGCN/Pd	B	10.5	2.78	Ethanol. HCl	>400$^{(3)}$	2.8	96	115
O-CCN/Pt	O	46.2	2.25	Naproxen	>420$^{(2)}$	0.88	1.27	116
CMCCN/Pt	O	46.2	2.72	TEOA	420$^{(2)}$	4.073	26.9	117
OKCN/Pt	O-K	45.4	2.71	TEOA	420$^{(2)}$	4.286	10.9	118
RPCN/Pt	C	13.8	1.71	TEOA	>300$^{(2)}$	2.95	21.1	119
K–I–CCN/Pt	J-K	78.1	2.62	TEOA	>400$^{(2)}$	5.12	4.83	120

Notes: Radiation sources: $^{(1)}$ – white light LED matrix, 50 Wt; $^{(2)}$ – Xe lamp, 300 Wt; $^{(3)}$ – Hg lamp, 1000 Wt. Other designations are the same as in the table. 1, 2.

Crystalline carbon nitride (APMCN) with the electron donor 4-amino-2,6-dihydroxypyrimidine (AP) embedded in the heptazine ring, and potassium ions and cyanide groups introduced into the structure of the material was synthesized by the ionothermic method based on the supramolecular complex of melamine with AP.[101] Due to the occurrence of an internal electric field, which contributed to the separation and movement of photogenerated charges, APMCN demonstrated 6 times higher photocatalytic activity in the process of obtaining hydrogen than bulk g-C_3N_4. Under optimal conditions, hydrogen evolved with a quantum yield of $\Phi = 62.8\%$ at $\lambda = 400$ nm (Table 3).

Carbon nitride doped with a rubidium ion (Rb-PCN) was synthesized by polycondensation of melamine at 600 °C in the presence of RbCl.[102] The optimized Rb-PCN demonstrated six times higher photocatalytic activity in the process of obtaining H_2 (Table 3) than bulk g-C_3N_4. Such functional properties of Rb-PCN are due to the restructuring of the material structure, which led to improved crystallinity, more intense light absorption, and more efficient separation of photogenerated charges.

By calcination at 550 °C for 2 h of bulk g-C_3N_4 in the presence of CsCl, cesium ion-doped CCN with a polyheptazinimide structure was obtained.[103] The synthesized CsCN-2h was tested as a photocatalyst for hydrogen evolution from TEOA solutions (Table 3) and demonstrated 23 times higher activity than bulk carbon nitride. This was facilitated by a large specific surface area, higher crystallinity, and significantly lower recombination efficiency of photogenerated electron-hole pairs.

Crystalline carbon nitride doped with sodium and potassium ions (K–Na–CCN) was obtained by treating a previously synthesized sample doped with sodium (Na–CCN) with a KOH solution.[104] K–Na–CCN with the participation of Pt NPs demonstrated the properties of a photocatalyst for the production of H_2 (Table 3). Its activity was significantly higher than that of bulk g-C_3N_4 and Na–CCN due to more intense light absorption and better separation and transfer of photogenerated charges.

CCN of tubular morphology with potassium, sodium, and lithium ions intercalated in its structure was synthesized by calcination at 500 °C of a mixture of melamine with LiCl + KCl + NaCl salts.[105] The localization of alkali metals in the CCN plane led to uneven charge distribution and the formation of an internal electric field. This contributed to the effective separation of photogenerated electron-hole pairs and the reduction of their recombination rate, which determined the high photocatalytic activity of the synthesized CNIC in the process of hydrogen evolution from TEOA solutions (Table 3). The reaction rate increased significantly when the reaction mixture was saturated with LiCl + KCl + NaCl salts. An increase in the rate of H_2 evolution in the presence of these salts, as in the literature,[96] may be due to an improvement in the dissociation of water molecules on the surface of the platinum co-catalyst and an increase in the rate of reduction of protons with the formation of hydrogen.

Alkaline earth metals. To improve the photocatalytic properties of CCN, it was also doped with alkaline earth metal ions. Thus, samples of crystalline carbon nitride doped with magnesium (MKCN), calcium (CKCN), strontium (SKCN), and barium (BKCN) ions were synthesized by the ionothermic method by polycondensation of urea in melts of KCl + MCl_2 salts (M = Mg, Ca, Sr, Ba) at 600 °C.[106] Doping with these metals led to an increase in the intensity of light absorption in the visible and near-IR range of the spectrum due to the appearance of the absorption band of the $n \rightarrow \pi^*$ electronic transition, as well as to an improvement in the mobility and conductivity of charge carriers and a decrease in their recombination efficiency. All this led to sufficiently high activity of the synthesized samples in the process of hydrogen evolution from TEOA solutions (Table 3). With the participation of the most active photocatalyst CKCN/Pt, hydrogen was formed with a quantum yield of Φ = 31.2, 4.8, 0.9, and 0.2% at λ = 420, 500, 600, and 700 nm, respectively.

Magnesium-doped potassium polyheptazinimide was obtained by treatment with a 5.7 M solution of $MgCl_2$ K-PHI, synthesized by calcination at 600 °C of 5-aminotetrazole in a LiCl + KCl melt.[107] This treatment of K-PHI led to the partial substitution of potassium ions for magnesium with the formation of CCN, which contained both metals in the structure. Synthesized Mg-K-PHI in the presence of deposited *in situ* Pt NPs demonstrated sufficiently high activity in the process of hydrogen evolution from TEOA solutions (Table 3), which was significantly higher than with the participation of K-PHI. In the same way, namely by treatment with a 5 M solution of $MgCl_2$ CCN, synthesized by calcination at 550 °C of bulk g-C_3N_4 in the eutectic mixture KCl + LiCl, magnesium and potassium doped crystalline carbon nitride (Mg-K-CGCN) was obtained.[108] The photocatalyst Mg-K-CGCN with the participation of the co-catalyst Pd/SiO_2 showed activity in the process of H_2 evolution from acidified ethanol-water solutions (Table 3), which was 60% higher than with the participation of g-C_3N_4. Such properties of Mg-K-CGCN can be associated with a change in the potentials of the allowed zones of CGCN due to the incorporation of Mg^{2+} ions into its structure, as well as an improvement in the separation of photogenerated charges, an increase in the efficiency of their transport and suppression of electron-hole recombination.

Other metals. In addition to alkali and alkaline earth metals, other metal dopants were also used to increase the photocatalytic activity of CCN. Thus, CCN doped with zinc was obtained by the two-stage ionothermic method, using melem, oligomelem, and melon synthesized in the first stage.[109] All Zn-CCN samples had a well-ordered crystal structure with an extended conjugation region in the heptazine layers and strongly absorbed light. With the participation of the optimal sample, hydrogen evolved from aqueous solutions of methanol with a quantum yield of Φ = 12.6% at λ = 420 nm (Table 3). CCN doped with zinc and potassium (Zn-K-CN) (Table 3), which was synthesized by calcining melamine in a $ZnCl_2$ + KCl melt at 600 °C, turned out to be a sufficiently active photocatalyst for the formation of H_2[110]. According to theoretical calculations, potassium ions are localized between layers of carbon nitride and create bridges between them, which improve the migration of charge carriers and suppress the recombination of photoexcited electron-hole pairs. At the same time, zinc ions occupy places inside the planes of heptazine. This promotes charge delocalization and extends the absorption range of visible light to 582 nm.

CCN based on triazine and heptazine, doped with nickel, was obtained by a two-step ionothermal method.[111]

The synthesized Ni-H/T-CCN demonstrated photocatalytic properties in the process of obtaining hydrogen from TEOA solutions (Table 3). With its participation, hydrogen evolved with a quantum yield of Φ = 7.8% at λ = 420 nm, which is 5.8 times higher than when using H/T-CCN. The high functional properties of Ni-H/T-CCN were due to the formation of a homojunction at the boundary of two isotypes of carbon nitride and effective separation of charges with its participation, as well as the presence of Ni atoms, which acted as active centers and exerted a certain influence on the strength of the internal electric field.

Crystalline carbon nitride doped with cobalt (Co-CCN) was significantly more active in the process of H_2 evolution from lactic acid solutions (Table 3).[112] To obtain it, the synthesized CCN was treated with a $CoCl_2$ solution under the influence of ultrasound. As experimental and theoretical studies have shown, cobalt atoms in Co-CCN are coordinated by four nitrogen atoms and one axial oxygen atom. The formed Co-N_4-O structures functioned as hole traps and enhanced the dissociation of photogenerated excitons.

Non-metals. Using urea and thiourea, a highly crystalline heterostructure based on isotypes of unmodified and sulfur-doped carbon nitride was obtained by a three-stage ionothermal method.[113] Due to the better separation of photogenerated charges, the synthesized CNF/SCNF-MS in the presence of deposited *in situ* Pt NPs demonstrated sufficiently high activity in the process of H_2 evolution from TEOA solutions (Table 3), which was significantly higher compared to the low-crystalline analog. Crystalline carbon nitride samples doped with sulfur (S-CGCN)[114] and boron (B-CGCN)[115] turned out to be effective photocatalysts for hydrogen evolution from acidified HCl water-ethanol solutions (Table 3). They were obtained, respectively, by heat treatment in a melt salts KCl + LiCl of S-g-C_3N_4, synthesized by pyrolysis of mixtures of melamine with S_8[114] and B-g-C_3N_4, synthesized by polycondensation of melamine in the presence of boric acid.[115] The photocatalytic activity of the synthesized S-CGCN and B-CGCN was significantly higher than that of undoped g-C_3N_4 and CGCN. This was due to more intense absorption of light, better separation of photogenerated charges, and suppression of their recombination.

Oxygen-doped CCN (O-CCN) was obtained by a two-stage ionothermal method using g-C_3N_4, synthesized by calcination of semicarbazide hydrochloride at 550 °C, followed by heat treatment in a KCl + LiCl melt.[116] The inclusion of O atoms in the CCN structure significantly expanded the visible light absorption range due to the emergence of the n→π* electronic transition band. Doping with oxygen also improved the separation of photogenerated charges and promoted the formation of H_2O_2 due to the formation of $OH^\bullet$ radicals – products of water decomposition. The synthesized O-CCN was tested as a photocatalyst for the simultaneous hydrogen evolution and the destruction of naproxen, ibuprofen, indomethacin, diclofenac sodium, and acetylsalicylic acid, which are typical wastewater pollutants in the production of these pharmaceuticals. Among the donors used, hydrogen was best evolved from naproxen solutions (Table 3).

A photocatalyst for hydrogen production (Table 3) based on oxygen-doped crystalline and amorphous carbon nitride with an internal homotransition was synthesized by a one-step method using melamine and cyanuric acid as precursors and KCl as a solid template.[117] With the participation of the optimally obtained CMCCN, H_2 evolved with a quantum yield of Φ = 26.9 and 14.0% at λ = 420 and 450 nm, respectively, which is 86 times higher than with the participation of bulk g-C_3N_4. Such properties of CMCCN were due to the narrowing of the band gap, which increased the intensity of absorption of visible light, and the presence of a homojunction, which ensured the effective separation and transfer of photogenerated charges. Due to the activation of a greater number of n→π* electronic transitions, it was possible to significantly expand the range of photosensitivity in the visible range of the spectrum (up to 650 nm) and increase the efficiency of hydrogen evolution using CCN doped with oxygen and potassium (OKCN) (Table 3).[118] It was synthesized by calcining a mixture of urea and oxalic acid in the presence of solid KCl.

Carbon-doped CCN (RPCN) synthesized by calcining a mixture of melamine and 2,4,6-triaminopyrimidine at 600 °C demonstrated photocatalytic activity in the process of hydrogen production (Table 3) under the influence of near-IR light.[119] Such CCN doping led to the localization of charge density and inhibition of radiative recombination of photogenerated electron-hole pairs. This, together with the intense absorption of light in the visible range of the spectrum, determined the high photocatalytic activity of RPCN/Pt in the process of hydrogen obtaining, which evolved with a quantum yield of Φ = 21.1 13, 1.74, and 0.8% at λ = 420, 500, 600, and 700 nm, respectively.

CCN doped with iodine and potassium (K–I–CCN) was active in the process of hydrogen release (Table 3).[120] It was obtained by heat treatment in a LiCl + KCl melt of bulk carbon nitride doped with iodine, synthesized by calcination of a mixture of DCDA, urea, and 1-ethyl-3-methylimidazole iodide.[120] Joint doping of CCN with these elements regulated the distribution of generated electron-hole pairs and the accumulation of surface charge, which determined the sufficiently high photocatalytic activity of K–I–CCN. With its participation and deposited *in situ* Pt NPs, hydrogen evolution was 7.3 times faster than when using bulk g-C_3N_4.

5. Conclusions

The photocatalytic systems considered in this review are based on crystalline graphitic carbon nitride – undoped with a controlled defective structure and doped with various metals and nonmetals, etc., testifying to the significant potential of this organic semiconductor for obtaining molecular hydrogen under the influence of light. At the same time, despite the successes achieved in laboratory studies of such processes with the participation of this semiconductor, it should be recognized that work in this field is at an initial stage. The systems tested today have several significant shortcomings, which do not yet allow us to talk about the possibility of practical implementation of hydrogen production processes using solar energy. In particular, this concerns the absence or extremely low activity of photocatalysts when they are excited by quanta of the near-IR range of the spectrum, where the intensity of solar radiation at the level of the earth's surface is the greatest. There are virtually no efficient CCN-based systems for complete photocatalytic water decomposition without the use of electron-donor-sacrifices. Further research is needed to clarify some other questions: i) a deeper understanding of the mechanism of formation of crystalline carbon nitride when using different methods, in particular, molten salt, which has found the widest application in the synthesis of CCN; ii) the influence of the morphology of CCN samples on their activity; iii) the role of structural defects, dopants, and functional groups in the processes of separation and migration of photogenerated charges; iv) detailed mechanisms of separation of electron-hole pairs formed under the action of light with the participation of heterostructures based on different isotypes of carbon nitride; v) stability of photocatalysts during their long-term operation, etc. Recommendations proposed when considering other photocatalytic systems based on graphitic carbon nitride[19,22-24,27] may also be useful.

Therefore, further efforts of scientists are needed to create significantly more effective photocatalysts based on crystalline carbon nitride, active under the action of light of a wide range of the spectrum, to find ways to overcome the identified shortcomings in the functioning of systems for obtaining hydrogen with the participation of this semiconductor.

Acknowledgements

This research was funded by the National Academy of Sciences of Ukraine under the project titled 'Development of fundamental principles for creating semiconductor nanostructures and nanocomposites for selective processes of photocatalytic and photoelectrocatalytic conversion of natural organic substances into important products' (№ 0122U201041).

References

[1] *Heterogeneous photocatalysis. From fundamentals to green applications*; Colmenares, J. C.; Xu, Y.-J., Eds.; Springer-Verlag GmbH, 2016. https://doi.org/10.1007/978-3-662-48719-8

[2] Kryukov, A. I.; Stroyuk, A. L.; Kuchmii, S. Ya.; Pokhodenko V. D. *Nanophotocatalysis*; Akademperiodika: Kyiv, 2013.

[3] Stroyuk, O. L.; Kuchmiy, S. Ya. Semiconductor Photocatalytic Systems for the Reductive Conversion of CO_2 and N_2: A Review. *Theor. Exp. Chem.* **2018**, *53*, 359–386. https://doi.org/10.1007/s11237-018-9535-0

[4] Ovcharov, M. L.; Mishura, A. M.; Shvalagin, V. V.; Granchak, V. M. Semiconductor Nanocatalysts for CO_2 Photoconversion Giving Organic Compounds: Design and Physicochemical Characteristics: A Review. *Theor. Exp. Chem.* **2019**, *55*, 2–28. https://doi.org/10.1007/s11237-019-09591-9

[5] Ovcharov, M. L.; Granchak, V. M. Photocatalytic Conversion of Nitrogen Oxides: Current State and Perspectives: A Review. *Theor. Exp. Chem.* **2021**, *57*, 30–63. https://doi.org/10.1007/s11237-021-09674-6

[6] Ovcharov, M. L.; Granchak, V. M. Photocatalytic Activation of Carbon Monoxide on Semiconductors and Derived Nanocomposites: Basic Principles and Mechanisms: A Review. *Theor. Exp. Chem.* **2019**, *55*, 173–200. https://doi.org/10.1007/s11237-019-09608-3

[7] Ali, S. H.; Mohammed, S. S.; Al-Dokheily, M. E.; Algharagholy, L. Photocatalytic Activity of Defective TiO_{2-x} for Water Treatment/Methyl Orange Dye Degradation. *Chem. Chem. Technol.* **2022**, *16*, 639–651. https://doi.org/10.23939/chcht16.04.639

[8] Affat, S. S.; Mohammed, S. S. Photocatalytic Degradation of Polyethylene Plastics Using $MgAl_2O_4$ Nanoparticles Prepared by Solid State Method. *Chem. Chem. Technol.* **2023**, *17*, 503–509. https://doi.org/10.23939/chcht17.03.503

[9] Stroyuk, O. L.; Kuchmiy, S. Ya. Heterogeneous Photocatalytic Selective Reductive Transformations of Organic Compounds: A Review. *Theor. Exp. Chem.* **2020**, *56*, 143–173. https://doi.org/10.1007/s11237-020-09648-0

[10] Kuchmiy, S. Ya.; Stroyuk, O. L. Selective Reductive Transformations of Organic Nitro Compounds in Heterogeneous Photocatalytic Systems: A Review. *Theor. Exp. Chem.* **2021**, *57*, 1–29. https://doi.org/10.1007/s11237-021-09673-7

[11] Bellardita, M.; Loddo, V.; Palmisano, L. Formation of High Added Value Chemicals by Photocatalytic Treatment of Biomass. Mini-Rev. *Org. Chem.* **2020**, *17*, 884–901. https://doi.org/10.2174/1570193X17666200131112856

[12] Cheng, Q.; Yuan, Y.-J. Tang, R.; Liu, Q.-Y.; Bao, L.; Wang, P.; Zhong, J.; Zhao, Z.; Yu, Z.-T.; Zou, Z. Rapid Hydroxyl Radical Generation on (001) Facets Exposed Ultrathin Anatase TiO_2 Nanosheets for Enhanced Photocatalytic Lignocelluloses-to-H_2 Conversion. *ACS Catal.* **2022**, *12*, 2118–2125. https://doi.org/10.1021/acscatal.1c05713

[13] Wang, X.; Maeda, K.; Thomas A.; Takanabe K.; Xin, G.; Carlsson, J. M.; Domen, K.; Antonietti, M. A Metal-Free Polymeric Photocatalyst for Hydrogen Production from Water Under Visible Light. *Nat. Mater.* **2009**, *8*, 76−80. https://doi.org/10.1038/nmat2317

[14] Maeda, K.; Wang, X.; Nishihara, Y.; Antonietti, M.; Domen, K. Photocatalytic Activities of Graphitic Carbon Nitride Powder for Water Reduction and Oxidation under Visible Light. *J. Phys. Chem. C* **2009**, *113*, 4940−4947. https://doi.org/10.1021/jp809119m

[15] Chen, X.; Jun, Y.-S.; Takanabe, K.; Maeda, K.; Domen, K.; Fu, X.; Antonietti, M.; Wang, X. Ordered Mesoporous SBA-15 Type Graphitic Carbon Nitride: A Semiconductor Host Structure for

Photocatalytic Hydrogen Evolution with Visible Light. *Chem. Mater*. **2009**, *21*, 4093–4095. https://doi.org/10.1021/cm902130z

[16] Wang, X.; Maeda, K.; Chen, X.; Takanabe, K.; Domen, K.; Hou, Y.; Fu, X.; Antonietti, M. Polymer Semiconductors for Artificial Photosynthesis: Hydrogen Evolution by Mesoporous Graphitic Carbon Nitride with Visible Light. *J. Am. Chem Soc*. **2009**, *131*, 1680–1681. https://doi.org/10.1021/ja809307s

[17] Ye, S.; Wang, R.; Wu, M.-Z.; Yuan, Y.-P. A Review on g-C$_3$N$_4$ for Photocatalytic Water Splitting and CO$_2$ Reduction. *Appl. Surf. Sci.* **2015**, *358 A*, 15–27. https://doi.org/10.1016/j.apsusc.2015.08.173

[18] Wen, J.; Xie, J.; Chen, X.; Li, X. A Review on g-C$_3$N$_4$-Based Photocatalysts. *Appl. Surf. Sci*. **2017**, *391*, 72–123. https://doi.org/10.1016/j.apsusc.2016.07.030

[19] Stroyuk, O. L.; Raevskaya, A. E.; Kuchmy, S. Ya. Photocatalytic Hydrogen Evolution under Visible Light Illumination in Systems Based on Graphitic Carbon Nitride: A Review. *Theor. Exp. Chem*. **2018**, *54*, 1–35. https://doi.org/10.1007/s11237-018-9541-2

[20] Singh, A. K.; Das, C.; Indra, A. Scope and Prospect of Transition Metal-Based Cocatalysts for Visible Light-Driven Photocatalytic Hydrogen Evolution with Graphitic Carbon Nitride. *Coord. Chem. Rev*. **2022**, *465*, 214516. https://doi.org/10.1016/j.ccr.2022.214516

[21] Hayat, A.; Syed, J. A. S.; Al-Sehemi, A. G.; El-Nasser, K. S.; Taha, T. A.; Al-Ghamdi, A. A.; Amin, M. A.; Ajmal Z.; Iqbal, W.; Palamanit, A.; *et al.* State of the Art Advancement in Rational Design of g-C$_3$N$_4$ Photocatalyst for Efficient Solar Fuel Transformation, Environmental Decontamination and Future Perspectives. *Int. J. Hydrogen En*. **2022**, *47*, 10837–10867. https://doi.org/10.1016/j.ijhydene.2021.11.252

[22] Stroyuk, A. L.; Raevskaya, A. E.; Kuchmy, S. Ya. Photocatalytic Selective Oxidation of Organic Compounds in Graphitic Carbon Nitride Systems: A Review. *Theor. Exp. Chem*. **2019**, *55*, 147–172. https://doi.org/10.1007/s11237-019-09607-4

[23] Kuchmiy, S. Ya.; Stroyuk, O. L. Photocatalytic Fixation of Molecular Nitrogen in Systems Based on Graphite-Like Carbon Nitride: A Review. *Theor. Exp. Chem*. **2021**, *57*, 85–112. https://doi.org/10.1007/s11237-021-09678-2

[24] Kuchmiy, S. Ya. Photocatalytic Air Decontamination from Volatile Organic Pollutants Using Graphite-Like Carbon Nitride: A Review. *Theor. Exp. Chem*. **2021**, *57*, 237–261. https://doi.org/10.1007/s11237-021-09693-3

[25] Wang, J.; Wang, S. A Critical Review on Graphitic Carbon Nitride (g-C$_3$N$_4$)-Based Materials: Preparation, Modification and Environmental Application. *Coord. Chem. Rev*. **2022**, *453*, 214338. https://doi.org/10.1016/j.ccr.2021.214338

[26] Akhundi, A.; Badiei, A.; Ziarani, G. M.; Habibi-Yangjeh, A.; Muñoz-Batista, M. J.; Luque, R. Graphitic Carbon Nitride-Based Photocatalysts: Toward Efficient Organic Transformation for Value-Added Chemicals Production. *Mol. Catal*. **2020**, *488*, 110902. https://doi.org/10.1016/j.mcat.2020.110902

[27] Kuchmiy, S. Ya. Photocatalytic Reforming of Biomass Components Using Systems Based on Graphite-Like Carbon Nitride: A Review. *Theor. Exp. Chem*. **2023**, *59*, 231–259. https://doi.org/10.1007/s11237-024-09783-y

[28] Jiang, L.; Yuan, X.; Pan, Y.; Liang, J.; Zeng, G.; Wu, Z.; Wang, H. Doping of Graphitic Carbon Nitride for Photocatalysis: A Review. *Appl. Catal. B*., **2017**, *217*, 388–406. https://doi.org/10.1016/j.apcatb.2017.06.003

[29] Patnaik, S.; Sahoo, D. P.; Parida, K. Recent Advances in Anion Doped g-C$_3$N$_4$ Photocatalysts: A Review. *Carbon*, **2020**, *172*, 682–711. https://doi.org/10.1016/j.carbon.2020.10.073

[30] Lee, C.-Y.; Zou, J.; Bullock, J.; Wallace G. G. Emerging Approach in Semiconductor Photocatalysis: Towards 3D Architectures for Efficient Solar Fuels Generation in Semi-Artificial Photosynthetic Systems. *J. Photochem. Photobiol. C*. **2019**, *39*, 142–160. https://doi.org/10.1016/j.jphotochemrev.2019.04.002

[31] He, F.; Wang, Z.; Li, Y.; Peng, S.; Liu B. The Nonmetal Modulation of Composition and Morphology of g-C$_3$N$_4$-Based Photocatalysts. *Appl. Catal. B*. **2020**, *269*, 118828. https://doi.org/10.1016/j.apcatb.2020.118828

[32] Stroyuk, O.; Raievska, O.; Zahn, D. R. T. Graphitic Carbon Nitride Nanotubes: A New Material for Emerging Applications. *RSC Adv*. **2020**, *10*, 34059–34087. https://doi.org/10.1039/D0RA05580H

[33] Li, Y.; He, Z.; Liu, L.; Jiang, Y.; Ong, W.-J.; Duan, Y.; Ho, W.; Dong, F. Inside-and-Out Modification of Graphitic Carbon Nitride (g-C$_3$N$_4$) Photocatalysts *via* Defect Engineering for Energy and Environmental Science. *Nano Energy* **2022**, *105*, 108032. https://doi.org/10.1016/j.nanoen.2022.108032

[34] Wang, W.; Shu, Z.; Liao, Z.; Zhou, J.; Meng, D.; Li, T.; Zhao, Z.; Xu L. Sustainable One-Step Synthesis of Nanostructured Potassium poly(Heptazine imide) for Highly Boosted Photocatalytic Hydrogen Evolution. *Chem. Eng. J*. **2021**, *424*, 130332. https://doi.org/10.1016/j.cej.2021.130332

[35] Lin, L.; Yu, Z.; Wang X. Crystalline Carbon Nitride Semiconductors for Photocatalytic Water Splitting. *Angew. Chem*. **2019**, *131*, 6225–6236. https://doi.org/10.1002/ange.201809897

[36] Lin, L.; Ou, H.; Zhang, Y.; Wang, X. Tri-s-Triazine-Based Crystalline Graphitic Carbon Nitrides for Highly Efficient Hydrogen Evolution Photocatalysis. *ACS Catal*. **2016**, *6*, 3921–3931. https://doi.org/10.1021/acscatal.6b00922

[37] Song, H.; Luo, L.; Wang, S.; Zhang, G.; Jiang B. Advances in poly(Heptazine imide)/poly(triazine imide) Photocatalyst. *Chin. Chem. Lett*. **2024**, *35*, 109347. https://doi.org/10.1016/j.cclet.2023.109347

[38] He, F.; Hu, Y.; Zhong, H.; Wang, Z.; Peng, S.; Li, Y. Effect of Molten-Salt Modulation on the Composition and Structure of g-C$_3$N$_4$-Based Photocatalysts. *Chem. Commun*. **2023**, *59*, 10476–10487. https://doi.org/10.1039/D3CC03052K

[39] Yan, B.; Chen, Z.; Xu, Y. Amorphous and Crystalline 2D Polymeric Carbon Nitride Nanosheets for Photocatalytic Hydrogen/Oxygen Evolution and Hydrogen Peroxide Production. *Chem. Asian J.* **2020**, *15*, 2329–2340. https://doi.org/10.1002/asia.202000253

[40] Wang, S.; Zhang, J.; Bin Li, B.; Sun, H.; Wang, S. Engineered Graphitic Carbon Nitride-Based Photocatalysts for Visible-Light-Driven Water Splitting: A Review. *En. Fuels* **2021**, *35*, 6504−6526. https://doi.org/10.1021/acs.energyfuels.1c00503

[41] Liu, J.; Fu, W.; Liao, Y.; Fan, J.; Xiang, Q. Recent Advances in Crystalline Carbon Nitride for Photocatalysis. *J. Mater. Sci. Technol*. **2021**, *91*, 224–240. https://doi.org/10.1016/j.jmst.2021.03.017

[42] Zhao, B.; Zhong, W.; Chen, F.; Wang, P.; Bie, C.; Yu, H. High-Crystalline g-C$_3$N$_4$ Photocatalysts: Synthesis, Structure Modulation, and H$_2$-Evolution Application. *Chin. J. Catal*. **2023**, *52*, 127–143. https://doi.org/10.1016/S1872-2067(23)64491-2

[43] Li, Y.; Ren, Z.; He, Z.; Ouyang, P.; Duan, Y.; Zhang, W.; Lv, K.; Dong, F. Crystallinity-Defect Matching Relationship of g-C$_3$N$_4$: Experimental and Theoretical Perspectives. *Green En. Environ*. **2024**, *9*, 623–658. https://doi.org/10.1016/j.gee.2023.02.012

[44] Li, H.; Cheng, B.; Xu, J.; Yu, J.; Cao, S. Crystalline Carbon Nitrides for Photocatalysis. *EES. Catal*. **2024**, *2*, 411–447. https://doi.org/10.1039/D3EY00302G

[45] Pu, W.; Zhou, Y.; Yang, L.; Gong, H.; Li, Y.; Yang, Q.; Zhang, D. High-Efficiency Crystalline Carbon Nitride Photocatalysts: Status and Perspectives. *Nano Res*. **2024**, *17*, 7840–7863. https://doi.org/10.1007/s12274-024-6818-8

[46] Zhang, Z.; Leinenweber, K.; Bauer, V.; Garvie, L. A. J.; McMillan, P. F.; Wolf, G. H. High-Pressure Bulk Synthesis of Crystalline $C_6N_9H_3$·HCl: A Novel C_3N_4 Graphitic Derivative. *J. Am. Chem. Soc*. **2001**, *123*, 7788–7796. https://doi.org/10.1021/ja0103849

[47] Kroke, E.; Schwarz, M. Novel Group 14 Nitrides. *Coord. Chem. Rev*. **2004**, *248*, 493–532. https://doi.org/10.1016/j.ccr.2004.02.001

[48] Horvath-Bordon, E.; Kroke, E.; Svobod, I.; Fuess, H.; Riedel, R. Potassium Melonate, $K_3[C_6N_7(NCN)_3]·5H_2O$, and its Potential Use for the Synthesis of Graphite-Like C_3N_4 Materials. *New J. Chem*. **2005**, *29*, 693–699. https://doi.org/10.1039/B416390G

[49] Sakata, Y.; Yoshimoto, K.; Kawaguchi, K.; Imamura, H.; Higashimoto S. Preparation of a Semiconductive Compound Obtained by the Pyrolysis of Urea under N_2 and the Photocatalytic Property under Visible Light Irradiation. *Catal. Today* **2011**, *161*, 41–45. https://doi.org/10.1016/j.cattod.2010.09.029

[50] Long B.; Lin J.; Wang, X. Thermally-Induced Desulfurization and Conversion of Guanidine Thiocyanate into Graphitic Carbon Nitride Catalysts for Hydrogen Photosynthesis. *J. Mater. Chem. A*. **2014**, *2*, 2942–2951. https://doi.org/10.1039/C3TA14339B

[51] Zhang, H.; Yu, A. Photophysics and Photocatalysis of Carbon Nitride Synthesized at Different Temperatures. *J. Phys. Chem. C* **2014**, *118*, 11628–11635. https://doi.org/10.1021/jp503477x

[52] Wang, C.; Xiao, H.; Lu, Y.; Lv, J.; Yuan, Z.; Cheng, J. Regulation of Polymerization Kinetics to Improve Crystallinity of Carbon Nitride for Photocatalytic Eactions. *ChemSusChem*. **2023**, *16*, e202300361. https://doi.org/10.1002/cssc.202300361

[53] Iqbal, W.; Qiu, B.; Zhu, Q.; Xing, M.; Zhang, J. Self-Modified Breaking Hydrogen Bonds to Highly Crystalline Graphitic Carbon Nitrides Nanosheets for Drastically Enhanced Hydrogen Production. *Appl. Catal. B* **2018**, *232*, 306–313. https://doi.org/10.1016/j.apcatb.2018.03.072

[54] Cheng, J.; Hu, Z.; Lv, K.; Wu, X.; Li, Q.; Li, Y.; Li, X.; Sun, J. Drastic Promoting the Visible Photoreactivity of Layered Carbon Nitride by Polymerization of Dicyandiamide at High Pressure. *Appl. Catal. B* **2018**, *232*, 330–339. https://doi.org/10.1016/j.apcatb.2018.03.066

[55] Yuan, Y. P.; Yin, L. S.; Cao, S. W.; Gu, L. N.; Xu, G. S.; Du, P.; Chai, H., Liao, Y. S.; Xue, C. Microwave-Assisted Heating Synthesis: A General and Rapid Strategy for Large-Scale Production of Highly Crystalline g-C_3N_4 with Enhanced Photocatalytic H_2 Production. *Green Chem*. **2014**, *16*, 4663–4668. https://doi.org/10.1039/C4GC01517G

[56] Guo, Y.; Li, J.; Yuan, Y.; Li, L.; Zhang, M.; Zhou, C.; Lin, Z. A Rapid Microwave-Assisted Thermolysis Route to Highly Crystalline Carbon Nitrides for Efficient Hydrogen Generation. *Angew. Chem*. **2016**, *128*, 14913–14917. https://doi.org/10.1002/ange.201608453

[57] Li, X.-H.; Zhang, J.; Chen, X.; Fischer, A.; Thomas, A.; Antonietti, M.; Wang, X. Condensed Graphitic Carbon Nitride Nanorods by Nanoconfinement: Promotion of Crystallinity on Photocatalytic Conversion. *Chem. Mater*. **2011**, *23*, 4344-4348. https://doi.org/10.1021/cm201688v

[58] Xing, W.; Tu, W.; Han, Z.; Hu, Y.; Meng, Q.; Chen G. Template-Induced High-Crystalline g-C_3N_4 Nanosheets for Enhanced Photocatalytic H_2 Evolution. *ACS En. Lett*. **2018**, *3*, 514-519. https://doi.org/10.1021/acsenergylett.7b01328

[59] Bhunia, M. K.; Melissen, S.; Parida, M. R.; Pradip Sarawade, P.; Basset, J.-M.; Anjum, D. H.; Mohammed, O. F.; Sautet, P.; Tangui Le Bahers, T. L.; Takanabe, K. Dendritic Tip-on Polytriazine-Based Carbon Nitride Photocatalyst with High Hydrogen Evolution Activity. *Chem. Mater*. **2015**, *27*, 8237–8247. https://doi.org/10.1021/acs.chemmater.5b02974

[60] Qiu, C.; Xu, Y.; Fan, X.; Xu, D.; Tandiana, R.; Ling, X.; Jiang, Y.; Liu, C.; Yu, L.; Chen, W.; *et al.* Highly Crystalline K-Intercalated Polymeric Carbon Nitride for Visible-Light Photocatalytic Alkenes and Alkynes Deuterations. *Adv. Sci*. **2019**, *6*, 1801403. https://doi.org/10.1002/advs.201801403

[61] Xu, Y.; He, X.; Zhong, H.; Singh, D. J.; Zhang, L.; Wang, R. Solid Salt Confinement Effect: An Effective Strategy to Fabricate High Crystalline Polymer Carbon Nitride for Enhanced Photocatalytic Hydrogen Evolution. *Appl. Cat. B* **2019**, *246*, 349–355. https://doi.org/10.1016/j.apcatb.2019.01.069

[62] Wang, W.; Shu, Z.; Zhou, J.; Meng, D. Alkali-Assisted Deep-Deamination to Improve the Crystallinity of poly(Heptazine imide) for Boosted Photocatalytic H_2 Evolution. *Separ. Purif. Technol*. **2023**, *318*, 124027. https://doi.org/10.1016/j.seppur.2023.124027

[63] Wang, W.; Shu, Z.; Zhou, J.; Meng, D.; Zhao, Z.; Li, T. Facile Synthesis and Microstructure Modulation of Crystalline Polymeric Carbon Nitride for Highly Boosted Photocatalytic Hydrogen Evolution. *J. Mater. Chem. A* **2020**, *8*, 6785–6794. https://doi.org/10.1039/D0TA01584A

[64] Wu, X.; Ma, H.; Zhong, W.; Fan, J.; Yu, H. Porous Crystalline g-C_3N_4: Bifunctional $NaHCO_3$ Template-Mediated Synthesis and Improved Photocatalytic H_2 Evolution Rate. *Appl. Catal. B* **2020**, *271*, 118899. https://doi.org/10.1016/j.apcatb.2020.118899

[65] Wu X.; Ma H.; Wang K.; Wang, J.; Wang, G.; Yu, H. High-Yield and Crystalline Graphitic Carbon Nitride Photocatalyst: One-Step Sodium Acetate-Mediated Synthesis and Improved Hydrogen-Evolution Performance. *J. Colloid and Interface Sci*. **2022**, *633*, 817–827. https://doi.org/10.1016/j.jcis.2022.11.143

[66] Xia, P.; Antonietti, M.; Zhu, B.; Heil, T.; Yu, J.; Cao, S. Designing Defective Crystalline Carbon Nitride to Enable Selective CO_2 Photoreduction in the Gas Phase. *Adv. Funct. Mater*. **2019**, *29*, 1900093. https://doi.org/10.1002/adfm.201900093

[67] Bojdys, M. J.; Muller, J. O.; Antonietti, M.; Thomas, A. Ionothermal Synthesis of Crystalline, Condensed, Graphitic Carbon Nitride. *Chem*. **2008**, *14*, 8177–8182. https://doi.org/10.1002/chem.200800190

[68] Chen, X.; Li, X.; Wu, J.; Fang, C.; Ding, J.; Wan, H.; Guan G. Boosting Photocatalytic H_2 Evolution by Ingenious Construction of Isotype Heptazine/Triazine Based Porous Carbon Nitride Heterojunction. *Separ. Purif. Technol*. **2022**, *297*, 121490. https://doi.org/10.1016/j.seppur.2022.121490

[69] Wirnhier, E.; Doblinger, M.; Gunzelmann, D.; Senker, J.; Lotsch, B. V.; Schnicket, W. Poly(Triazineimide) with Intercalation of Lithium and Chloride Ions $[(C_3N_3)_2(NH_xLi_{1-x})_3·LiCl]$: A Crystalline 2D Carbon Nitride Network. *Chem*. **2011**, *17*, 3213–3221. https://doi.org/10.1002/chem.20100246

[70] Schwinghammer, R.; Tuffy, B.; Mesch, M. B.; Wirnhier, E.; Martineau, C.; Taulelle, F.; Schnick, W.; Senker, J.; Lotsch, B. V. Triazine-Based Carbon Nitrides for Visible-Light-Driven Hydrogen Evolution. *Angew. Chem. Int. Ed*. **2013**, *52*, 2435–2439. https://doi.org/10.1002/anie.201206817

[71] Ham, Y.; Maeda, K.; Cha, D.; Takanabe, K.; Domen, K. Synthesis and Photocatalytic Activity of poly (triazine imide). *Chem. Asian J*. **2013**, *8*, 218–224. https://doi.org/10.1002/asia.201200781

[72] He, F.; Wang, M.; Luo, L.; Wang, Z.; Peng, S.; Li, Y. Directional Modulation of Triazine and Heptazine Based Carbon Nitride for Efficient Photocatalytic H_2 Evolution. *Appl. Surf. Sci*. **2021**, *562*, 150103. https://doi.org/10.1016/j.apsusc.2021.150103

[73] Li, Y.; Zhang, D.; Fan, J.; Xiang, Q. Highly Crystalline Carbon Nitride Hollow Spheres with Enhanced Photocatalytic Performance. *Chin. J. Catal*. **2021**, *42*, 627–636. https://doi.org/10.1016/S1872-2067(20)63684-1

[74] An, W.; Zhi, X.; Zhai, B.; Niu, P.; Wang, S.; Li, L. Crystallinity Improvement of poly(Heptazine imide) for High Photocatalytic

Hydrogen Evolution. *Scripta Mater*. **2022**, *221*, 114992. https://doi.org/10.1016/j.scriptamat.2022.114992

[75] Wang, S.; He, F.; Lu, Y.; Wu, Y.; Zhang, Y.; Dong, P.; Liu, X.; Zhao, C.; Wang, S.; Wang, D.; *et al*. Enhancing Photocatalytic Hydrogen Production of Carbon Nitride: Dominant Advantage of Crystallinity over Mass Transfer. *J. Colloid and Interface Sci*. **2024**, *654 A*, 317–326. https://doi.org/10.1016/j.jcis.2023.10.046

[76] Yu, Z.; Yue, X.; Fan, J.; Xiang, Q. Crystalline Intramolecular Ternary Carbon Nitride Homojunction for Photocatalytic Hydrogen Evolution. *ACS Catal*. **2022**, *12*, 6345–6358. https://doi.org/10.1021/acscatal.2c01563

[77] Wu, Z.; Gao, H.; Yan, S.; Zou Z. Synthesis of Carbon Black/Carbon Nitride Intercalation Compound Composite for Efficient Hydrogen Production. *Dalton Trans*. **2014**, *43*, 12013–12017. https://doi.org/10.1039/C4DT00256C

[78] Jin, A.; Jia, Y.; Chen, C.; Liu, X.; Jiang, J.; Chen, X.; Zhang, F. Efficient Photocatalytic Hydrogen Evolution on Band Structure Tuned Polytriazine/Heptazine Based Carbon Nitride Heterojunctions with Ordered Needle-Like Morphology Achieved by an *in situ* Molten Salt Method. *J. Phys. Chem. C* **2017**, *121*, 21497–21509. https://doi.org/10.1021/acs.jpcc.7b07243

[79] Zhao, Z.; Shu, Z.; Zhou, J.; Li, T.; Yan, F.; Wang, W.; Xu, L.; Shi, L.; Liao, Z. One-Step Fabrication of Crystalline Carbon Nitride with Tunable in-Plane/Interlayer Crystallinity for Enhanced Photocatalytic Hydrogen Evolution. *J. Alloys and Compounds* **2022**, *910*, 164828. https://doi.org/10.1016/j.jallcom.2022.164828

[80] Liu, H.; Chen, D.; Wang, Z.; Jing, H.; Zhang, R. Microwave-Assisted Molten-Salt Rapid Synthesis of Isotype Triazine-/Heptazine Based g-C_3N_4 Heterojunctions with Highly Enhanced Photocatalytic Hydrogen Evolution Performance. *Appl. Catal. B* **2017**, *203*, 300–313. https://doi.org/10.1016/j.apcatb.2016.10.014

[81] Liu, J.; Fang, W.; Wei, Z.; Qin, Z.; Jiang, Z.; Shangguan, W. Efficient Photocatalytic Hydrogen Evolution on N-Deficient g-C_3N_4 Achieved by a Molten Salt Post-Treatment Approach. *Appl. Catal. B* **2018**, *238*, 465–470. https://doi.org/10.1016/j.apcatb.2018.07.021

[82] Chen, C. C.; Tsai, D. L.; Liu, H. T.; Wu J. J. Carbon Vacancy-Modified Carbon Nitride Allotropic Composite for Solar Hydrogen Generation Coupled with Selective Oxidation of 5-Hydroxymethylfurfural. *ACS Sustain. Chem. Eng*. **2023**, *11*, 6435–6444. https://doi.org/10.1021/acssuschemeng.3c00363

[83] Ren, W.; Cheng, J.; Ou, H.; Huang, C.; Titirici, M.-M.; Wang, X. Enhancing Visible-Light Hydrogen Evolution Performance of Crystalline Carbon Nitride by Defect Engineering. *ChemSusChem*. **2019**, *12*, 3257–3262. https://doi.org/10.1002/cssc.201901011

[84] Deng, P.; Liu, Y.; Shi, L.; Cui, L.; Si, W.; Yao, L. Enhanced Visible-Light H_2 Evolution Performance of Nitrogen Vacancy Carbon Nitride by Improving Crystallinity. *Optic Mater*. **2021**, *120*, 111407. https://doi.org/10.1016/j.optmat.2021.111407

[85] Shao, Y.; Hao, X.; Lu, S.; Jin, Z. Molten Salt-Assisted Synthesis of Nitrogen-Vacancy Crystalline Graphitic Carbon Nitride with Tunable Band Structures for Efficient Photocatalytic Overall Water Splitting. *Chem. Eng. J*. **2023**, *454 Part 1*, 140123. https://doi.org/10.1016/j.cej.2022.140123

[86] Deng, H.; Jia, Y.; Wang, W.; Zhong, S.; Hao, R.; Fan, L.; Liu, X. Defect and Crystallinity-Mediated Charge Separation in Carbon Nitride for Synergistically Boosted Solar-Driven Hydrogen Evolution. *ACS Sustain. Chem. Eng*. **2023**, *11*, 13736–13746. https://doi.org/10.1021/acssuschemeng.3c03772

[87] Wang, Y. X.; Rao, L.; Wang, P. F.; Guo, Y.; Shi, Z. Y.; Guo, X.; Zhang, L. X. Synthesis of Nitrogen Vacancies g-C_3N_4 with Increased Crystallinity under the Controlling of Oxalyl Dihydrazide: Visible-Light-Driven Photocatalytic Activity. *Appl. Surf. Sci*. **2020**, *505*, 144576. https://doi.org/10.1016/j.apsusc.2019.144576

[88] Wang, W.; Kou, X.; Li, T.; Zhao, R.; Su, Y. Tunable Heptazine/Triazine Feature of Nitrogen Deficient Graphitic Carbon Nitride for Electronic Modulation and Boosting Photocatalytic Hydrogen Evolution. *J. Photochem. Photobiol. A* **2023**, *435*, 114308. https://doi.org/10.1016/j.jphotochem.2022.114308

[89] Chen, L.; Ning, S.; Liang, R.; Xia, Y.; Huang, R.; Yan, G.; Wang, X. Potassium Doped and Nitrogen Defect Modified Graphitic Carbon Nitride for Boosted Photocatalytic Hydrogen Production. *Int. J. Hydrogen En*. **2022**, *47*, 14044–14052. https://doi.org/10.1016/j.ijhydene.2022.02.147

[90] Yu, H.; Ma, H.; Wu, X.; Wang, X.; Fan, J.; Yu, J. One-Step Realization of Crystallization and Cyano-Group Generation for g-C_3N_4 Photocatalysts with Improved H_2 Production. *Sol. RRL* **2020**, *5*, 2000372. https://doi.org/10.1002/solr.202000372

[91] Yuan, J.; X. Liu, X.; Tang, Y.; Zeng, Y.; Wang, L.; Zhang, S.; Cai, T.; Liu, Y.; Luo, S.; Pei, Y.; *et al*. Positioning Cyanamide Defects in g-C_3N_4: Engineering Energy Levels and Active Sites for Superior Photocatalytic Hydrogen Evolution. *Appl. Catal. B* **2018**, *237*, 24–31. https://doi.org/10.1016/j.apcatb.2018.05.064

[92] Deng, P.; Shi, L.; Wang, H.; Qi, W. One-Step Preparation of Novel K^+ and Cyano-Group co-Doped Crystalline Polymeric Carbon Nitride with Highly Efficient H_2 Evolution. *Colloids and Surfaces A* **2020**, *601*, 125023. https://doi.org/10.1016/j.colsurfa.2020.125023

[93] Zhao, B.; Gao, D.; Liu, Y.; Fan, J.; Yu, H. Cyano Group-Enriched Crystalline Graphitic Carbon Nitride Photocatalyst: Ethyl Acetate-Induced Improved Ordered Structure and Efficient Hydrogen-Evolution Activity. *J. Colloid Interface Sci*. **2022**, *608 Part 2*, 1268–1277. https://doi.org/10.1016/j.jcis.2021.10.108

[94] Yang, S.; Zhang, H.; Wang, J.; Xiang, J.; Fu, Z.; Wang, Y.; Li, Z.; Xie, H.; Tang, S.; Li, Y. Spatially Restricted Strategy to Construct Crystalline Carbon Nitride Nanosheet Assists Exciton Dissociation to Enhance Photocatalytic Hydrogen Evolution Activity. *Appl. Surf. Sci*. **2023**, *616*, 156523. https://doi.org/10.1016/j.apsusc.2023.156523

[95] Yuan, J.; Tang, Y.; Yi, X.; Liu, C.; Li, C.; Zeng, Y.; Luo, S. Crystallization, Cyanamide Defect and Ion Induction of Carbon Nitride: Exciton Polarization Dissociation, Charge Transfer and Surface Electron Density for Enhanced Hydrogen Evolution. *Appl. Catal. B* **2019**, *251*, 206–212. https://doi.org/10.1016/j.apcatb.2019.03.069

[96] Teixeira, I. F.; Tarakina, N. V.; Silva, I. F.; López-Salas, N.; Savateev, A.; Antonietti, M. Overcoming Electron Transfer Efficiency Bottlenecks for Hydrogen Production in Highly Crystalline Carbon Nitride-Based Materials. *Adv. Sustain. Syst*. **2022**, *6*, 2100429. https://doi.org/10.1002/adsu.202100429

[97] Xu, C.; Liu, H.; Wang, D.; Li, D.; Zhang, Y.; Liu, X.; Huang, J.; Wu, S.; Fan, D.; Liu, H.; *et al.* Molten-Salt Assisted Synthesis of Polymeric Carbon Nitride-Based Photocatalyst for Enhanced Photocatalytic Activity under Green Light Irradiation. *Appl. Catal. B* **2023**, *334*, 122835. https://doi.org/10.1016/j.apcatb.2023.122835

[98] Chen, Z.; Savateev, A.; Pronkin, S.; Papaefthimiou, V.; Wolff, C.; Willinger, M. G.; Willinger, E.; Neher, D.; Antonietti, M.; Dontsova, D. "The Easier the Better" Preparation of Efficient Photocatalysts-Metastable poly(Heptazine imide) Salts. *Adv. Mater*. **2017**, *29*, 1700555. https://doi.org/10.1002/adma.201700555

[99] Zhang, G.; Xu, Y.; Yan, D.; He, C.; Li, Y.; Ren, X.; Zhang, P.; Mi, H. Construction of K^+ Ion Gradient in Crystalline Carbon Nitride to Accelerate Exciton Dissociation and Charge Separation for Visible Light H_2 Production. *ACS Catal*. **2021**, *11*, 6995–7005. https://doi.org/10.1021/acscatal.1c00739

[100] Lin, L.; Ren, W.; Wang, C.; Asiri, A. M.; Zhang, J.; Wang, X. Crystalline Carbon Nitride Semiconductors Prepared at Different Temperatures for Photocatalytic Hydrogen Production. *Appl. Cat. B* **2018**, *231*, 234–241. https://doi.org/10.1016/j.apcatb.2018.03.009

[101] Zeng, W.; Dong, Y.; Ye, X.; Zhang, Z.; Zhang, T.; Guan, X.; Guo, L. Crystalline Carbon Nitride with in-Plane Built-in Electric Field Accelerates Carrier Separation for Excellent Photocatalytic Hydrogen Evolution. *Chin. Chem. Lett*. **2024**, *35*, 109252. https://doi.org/10.1016/j.cclet.2023.109252

[102] Xu, Y.; Shi, W.; Zhang, Y.; Tu, Z.; Sun, B.; Wang, Z.; Wang, X.; Liu, Z.; Wang, W. Realigning the Melon Chains in Carbon Nitride by Rubidium Ions to Promote Photo-Reductive Activities for Hydrogen Evolution and Environmental Remediation. *J. Hazard. Mater*. **2023**, *453*, 131435. https://doi.org/10.1016/j.jhazmat.2023.131435

[103] Xu, W.; An, X.; Zhang, Q.; Li, Z.; Zhang, Q.; Yao, Z.; Wang, X.; Wang, S.; Zheng, J.; Zhang, J.; *et al*. Cesium Salts as Mild Chemical Scissors to Trim Carbon Nitride for Photocatalytic H_2 Evolution. *ACS Sustain. Chem. Eng*. **2019**, *7*, 12351−12357. https://doi.org/10.1021/acssuschemeng.9b01717

[104] Liao, Z.; Li, C.; Shu, Z.; Zhou, J.; Li, T.; Wang, W.; Zhao, Z.; Xu, L.; Shi, L.; Feng, L. K–Na co-Doping in Crystalline Polymeric Carbon Nitride for Highly Improved Photocatalytic Hydrogen Evolution. *Int. J. Hydrogen En*. **2021**, *46*, 26318–26328. https://doi.org/10.1016/j.ijhydene.2021.05.138

[105] Gao, H.; Yan, S.; Wang, J.; Huang, Y. A.; Wang, P.; Li, Z.; Zou, Z. Towards Efficient Solar Hydrogen Production by Intercalated Carbon Nitride Photocatalyst. *Phys. Chem. Chem. Phys*. **2013**. *15*, 18077–18084. https://doi.org/10.1039/C3CP53774A

[106] Zhang, G.; Xu, Y.; Rauf, M.; Zhu, J.; Li, Y.; He, C.; Ren, X.; Zhang, P.; Mi, H. Breaking the Limitation of Elevated Coulomb Interaction in Crystalline Carbon Nitride for Visible And Near-Infrared Light Photoactivity. *Adv. Sci*. **2022**, *9*, 2201677. https://doi.org/10.1002/advs.202201677

[107] Sahoo, S. K.; Teixeira, I. F.; Naik, A.; Heske, J.; Cruz, D.; Antonietti, M.; Savateev, A.; Kühne, T. D. Photocatalytic Water Splitting Reaction Catalyzed by Ion-Exchanged Salts of Potassium poly(Heptazine imide) 2D Materials. *J. Phys. Chem. C*. **2021**, *125*, 13749–13758. https://doi.org/10.1021/acs.jpcc.1c03947

[108] Grodzyuk G. Ya.; Koryakina K. V.; Shvalagin V. V.; Korzhak, G.V.; Kuchmiy, S.Y. Photocatalytic Evolution of Hydrogen from Alcohol–Aqueous Solutions Using Nanocrystalline Carbon Nitride Modified with Magnesium Chloride under the Visible Light Irradiation. *Theor. Exp. Chem*. **2022**, *58*, 198–204. https://doi.org/10.1007/s11237-022-09736-3

[109] Wang, Y.; Zhou, X.; Xu, W.; Sun, Y.; Wang, T.; Zhang, Y.; Dong, J.; Hou, W.; Wu, N.; Wu, L.; *et al*. Zn-Doped Tri-S-Triazine Crystalline Carbon Nitrides for Efficient Hydrogen Evolution Photocatalysis. *Appl. Catal. A* **2019**, *582*, 117118. https://doi.org/10.1016/j.apcata.2019.117118

[110] Wu, Y.; Xu, W.; W, N.; Wang, Z.; Wang, Y.; Zhang, Y.; Zhong, W.; Cai, H. L.; Wu, X. S. Bridging and Bonding: Zinc and Potassium co-Assisted Crystalline g-C_3N_4 for Significant Highly Efficient upon Photocatalytic Hydrogen Evolution. *Appl. Surf. Sci*. **2021**, *542*, 148620. https://doi.org/10.1016/j.apsusc.2020.148620

[111] Shi, W.; Cao, L.; Shi, Y.; Zhong, W.; Chen, Z.; Wei, Y.; Guo, F.; Chen, L.; Du, X. Boosted Built-in Electric Field and Active Sites Based on Ni-Doped Heptazine/Triazine Crystalline Carbon Nitride for Achieving High-Efficient Photocatalytic H_2 Evolution. *J. Mol. Str*. **2023**, *1280*, 135076. https://doi.org/10.1016/j.molstruc.2023.135076

[112] Wang Y.; Xie D.; Wang G.; Wu, Y.; Shi, R.; Zhou, C.; Meng, X.; Zhang, T. Single-Atomic Co-N_4-O Site Boosting Exciton Dissociation and Hole Extraction for Improved Photocatalytic Hydrogen Evolution in Crystalline Carbon Nitride. *Nano En*. **2022**, *104, Part A*, 107938. https://doi.org/10.1016/j.nanoen.2022.107938

[113] Xu, T.; Xia, Z.; Li, H.; Niu, P.; Wang, S.; Li, L. Constructing Crystalline g-C_3N_4/g-$C_3N_{4-x}S_x$ Isotype Heterostructure for Efficient Photocatalytic and Piezocatalytic Performances. *En. Environ. Mater*. **2023**, *6*, e12306. https://doi.org/10.1002/eem2.12306

[114] Ovcharov, M. L.; Glukhova, P. I.; Korzhak, G. V.; Kutsenko, O. S.; Stara, T. R.; Kuchmiy, S. Ya. Influence of Sulfur Doping of Crystalline Carbon Nitride on Photocatalytic Hydrogen Evolution from Alcohol–Aqueous Solutions under Visible Light. *Theor. Exp. Chem*. **2024**, *59*, 397–405. https://doi.org/10.1007/s11237-024-09798-5

[115] Stara, T.; Kutsenko, A.; Korzhak, H.; Ovcharov, M.; Kuchmiy, S. Photocatalytic Activity of Boron-Doped Bulk and Crystalline Graphitic Carbon Nitride in Visible Light-Driven Hydrogen Production. *Chem. Chem. Technol*. **2024**, *18*, 449–457. https://doi.org/10.23939/chcht18.04.449

[116] Wang, Y.; Zhou, J.; Wang, F.; Xie, Y.; Liu, S.; Ao, Z.; Li, C. Hydrogen Generation from Photocatalytic Treatment of Wastewater Containing Pharmaceuticals and Personal Care Products by Oxygen-Doped Crystalline Carbon Nitride. *Separ. Purif. Technol*. **2022**, *296*, 121425. https://doi.org/10.1016/j.seppur.2022.121425

[117] Li, J.; Liu, X.; Che, H.; Liu, C.; Li, C. Facile Construction of O-Doped Crystalline/Non-Crystalline g-C_3N_4 Embedded Nano-Homojunction for Efficiently Photocatalytic H_2 Evolution. *Carbon* **2021**, *172*, 602–612. https://doi.org/10.1016/j.carbon.2020.10.051

[118] Zhang, G.; Xu, Y.; He, C.; Zhang, P.; Mi, H. Oxygen-Doped Crystalline Carbon Nitride with Greatly Extended Visible-Light-Responsive Range for Photocatalytic H_2 Generation. *Appl. Catal. B* **2021**, *283*, 119636. https://doi.org/10.1016/j.apcatb.2020.119636

[119] Xu, Y.; Fan, M.; Yang, W.; Xiao, Y.; Zeng, L.; Wu, X.; Xu, Q.; Su, C.; He, Q. Homogeneous Carbon/Potassium-Incorporation Strategy for Synthesizing Red Polymeric Carbon Nitride Capable of Near-Infrared Photocatalytic H_2 Production. Adv. Mater. 2021, 33, 2101455. https://doi.org/10.1002/adma.202101455

[120] Cui, Y.; Li, X.; Yang, C.; Xiao, B.; Xu, H. K–I co-Doped Crystalline Carbon Nitride with Outstanding Visible Light Photocatalytic Activity for H_2 Evolution. *Int. J. Hydrogen En*. **2022**, *47*, 12569–12581. https://doi.org/10.1016/j.ijhydene.2022.02.005

Received: September 22, 2024 / Revised: November 22, 2024 / Accepted: December 01, 2024

ФОТОКАТАЛІТИЧНІ СИСТЕМИ НА ОСНОВІ КРИСТАЛІЧНОГО НІТРИДУ ВУГЛЕЦЮ ДЛЯ ОДЕРЖАННЯ ВОДНЮ

Анотація. *Розглянуто сучасний стан досліджень фотокаталітичних систем на основі кристалічного графітоподібного нітриду вуглецю (CCN) для виділення H_2 з водних розчинів електронодонорних субстратів. Обговорено методи синтезу CCN і фотокаталітичні властивості різних зразків CCN – нелегованих з контрольованою структурою дефектів і легованих металами та неметалами. Окреслено можливі напрямки подальших досліджень таких фотокаталітичних систем на основі CCN.*

Ключові слова: *кристаліний нітрид вуглецю, фотокаталіз, молекулярний водень.*